5-2020

IMPACT OF EPA AND DHA SUPPLEMENTATION AND 15-LOX-1 EXPRESSION ON COLITIS AND COLITIS-ASSOCIATED COLORECTAL CANCER

Jonathan Jaoude

IMPACT OF EPA AND DHA SUPPLEMENTATION AND 15-LOX-1 EXPRESSION ON COLITIS AND COLITIS-ASSOCIATED COLORECTAL CANCER

by

Jonathan Jaoude, B.S., M.A.

APPROVED:

Imad Shureiqi
_____
Imad Shureiqi, M.D., M.S.
Advisory Professor

Peiying Yang
_____
Peiying Yang, M.S., Ph.D.

David Volk
_____
David Volk, Ph.D.

Donghui Li
_____
Donghui Li, Ph.D

Kimberly Schluns
_____
Kimberly Schluns, Ph.D.

APPROVED:

_____
Dean, The University of Texas
MD Anderson Cancer Center UTHealth Graduate School of Biomedical Sciences

IMPACT OF EPA AND DHA SUPPLEMENTATION AND 15-LOX-1 EXPRESSION ON COLITIS AND COLITIS-ASSOCIATED COLORECTAL CANCER

A

THESIS

Presented to the Faculty of

The University of Texas

MD Anderson Cancer Center UTHealth

Graduate School of Biomedical Sciences

in Partial Fulfillment

of the Requirements

for the Degree of

MASTER OF SCIENCE

by

Jonathan Jaoude, B.S., M.A.

Houston, Texas

May 2020

IMPACT OF EPA AND DHA SUPPLEMENTATION AND 15-LOX-1 EXPRESSION ON COLITIS AND COLITIS-ASSOCIATED COLORECTAL CANCER

Jonathan Jaoude, B.S., M.A.

Advisory Professor: Imad Shureiqi, M.D., M.S.

ABSTRACT: Inflammatory bowel disease (IBD) patients not only suffer from colitis but also from increased morbidity and mortality of colitis-associated colorectal cancer (CAC). The enzyme 15-lipoxygenase-1 (15-LOX-1) is crucial to converting omega-3 fatty acid derivatives eicosapentaenoic acid (EPA) and docosahexaenoic acid (DHA) to resolvins, potent anti-inflammatory products. 15-LOX-1 effects on the conversion of EPA and DHA to resolvins that subsequently exert anti-inflammatory and anti-tumorigenic effects have received little attention. To address this knowledge gap, we hypothesize that 15-LOX-1 expression in colonic epithelial cells is essential for resolvin biosynthesis from EPA and DHA to modulate immunophenotype, limit inflammation, promote resolution, and help prevent colitis and CAC. Mice were treated with dextran sodium sulfate (DSS) alone only to induce acute and chronic colitis, or with DSS following an azoxymethane injection to induce CAC. In the chronic colitis model, DHA diet and/or expression of 15-LOX-1 reduced inflammation and altered immune cell populations. In the CAC model, DHA reduces tumor numbers by 54% in the WT/DHA group and by 52% in the 15-LOX-1/DHA group. Increased levels of 17-HDHA, RvD1, RvD4, and RvD5 in the 15-LOX-1/DHA group were inversely correlated to tumor number. EPA diet with and without expression of 15-LOX-1 reduced tumors by 47-48%. In conclusion, our study strongly supports the critical role of 15-LOX-1 for RvD production from DHA. CAC suppression occurred with DHA supplementation with and without 15-LOX-1 transgenic expression and seems to be less dependent on the production of RvDs. Further in-depth mechanistic studies are therefore needed to be better define the role of resolvins in CAC and colonic tumorigenesis in general.

Table of Contents

List of Illustrations

List of Tables

Abbreviations: colorectal cancer (CRC), colitis-associated colorectal cancer (CAC), inflammatory bowel disease (IBD), polyunsaturated fatty acid (PUFA), azoxymethane (AOM), dextran sodium sulfate (DSS), docosahexaenoic acid (DHA), eicosapentaenoic acid (EPA), E/D-series resolvins (RvE/D), 15-lipoxygenase-1 (15-LOX-1).

1. Introduction

Colorectal cancer (CRC) is the third most commonly diagnosed cancer and the fourth leading cause of cancer death in the world (1). Inflammatory bowel disease (IBD) patients not only suffer from colitis but also from increased morbidity and mortality for colitis-associated colorectal cancer (CAC). A global meta-analysis measured a 0.3% incidence rate per year for CAC (2), and a CRC prevalence of 3.7% with colitis patients (3). Though the incidence rate and prevalence of CAC seem low, IBD is the third highest risk factor for developing CRC. An estimated 10-15% of deaths in IBD patients are related to colorectal cancer (4). Evidently, it is important to treat IBD as a preventative measure to reduce CAC.

Fish oil and its omega-3 polyunsaturated fatty acid (PUFA) derivatives eicosapentaenoic acid (EPA) and docosahexaenoic acid (DHA) are widely promoted as agents that prevent chronic inflammation and cancer. EPA and DHA are also approved by the U.S. Food and Drug Administration (FDA) for treatments of hyperlipidemia (5). However, the effects of fish oils and omega-3 PUFAs on cancer are polarized between beneficial and harmful (6, 7). EPA inhibited polyp formation in a randomized clinical trial with familial adenomatous polyposis patients (8). Intraperitoneal treatment with 17-HDHA, a DHA derivative, has been seen to reduce colon epithelial damage and macrophage infiltration in a DSS mouse model (9). On the contrary, fish oils enriched with DHA induced severe colitis and adenocarcinoma formation in SMAD3-/- mice (10).

Chronic inflammation mechanistically promotes CRC; halting chronic inflammation could help prevent tumorigenesis (11, 12). Oxidative metabolites of EPA and DHA, resolvin E series (e.g., RvE1) derived from EPA and resolvin D series (e.g., RvD1) from DHA, are among the most studied pro-resolving mediators (13-17). Endogenous EPA can be converted to three known resolvins, RvE1-E3, and DHA to six known resolvins, RvD1-D6 (18). RvE1 displayed

potent anti-inflammatory actions on colitis (19) and attenuates TNF-stimulated nuclear factor-κB activation (20). In DSS-induced colitis mice, RvD1 and RvD2 prevent colitis by suppressing major pro-inflammatory mediators (TNF-α, IL-1β, and NF-κB, etc.) and reducing colon damage (21). RvD5 reduced neutrophil recruitment in intestinal ischemia reperfusion injury, therefore, protecting tissue and enhancing resolution (22).

The enzyme 15-lipoxygenase-1 (15-LOX-1) is crucial in converting EPA and DHA to potent anti-inflammatory resolvins (23). The RvE precursor, 18-HEPE, is catalyzed by aspirin-acetylated COX-2, a functionally similar enzyme to 15-LOX-1 (24). RvD precursor, 17-S-HpDHA, is generated from DHA by 15-LOX-1 (25, 26). 15-LOX-1 has been widely shown to promote inflammation resolution in various experimental models (27). The enzyme is downregulated in human cancers of the lung (28), esophagus (29), breast (30), endometrium (31), urinary bladder (32), pancreas (33), and especially the colon (34-37). In addition, 15-LOX-1 is repressed in 128 human cancer cell lines representing 20 different human cancer types (28). Repressed 15-LOX-1 is transcriptionally mediated (38) and independent of substrate availability (39). More recently, 15-LOX-1 was established to hold a tumor suppressive role, especially in colorectal tumorigenesis (23, 40). Re-expression of 15-LOX-1 in colorectal cancer cells via pharmaceutical agents, plasmids, or adenoviral vectors inhibited cancer cells from growing in vitro and in vivo (35, 41-46). Expression of human 15-LOX-1 in mouse epithelial colon cells inhibited colorectal tumorigenesis (43) and colitis-associated colorectal tumorigenesis (47, 48).

However, 15-LOX-1 effects on EPA and DHA modulating anti-inflammatory and anti-tumorigenic mediators have received little if any research attention. In our preliminary studies, EPA anti-tumorigenic effects on AOM/DSS-induced colorectal cancer were dependent not only on the availability of the substrate but also on the activity of the initial oxidative metabolizing

enzyme, 15-LOX-1, and subsequent resolvin generation. Interestingly, more preliminary studies show that DHA without 15-LOX-1 might lose anti-tumorigenic effects.

More specifically, limited attention has been placed on the effects of 15-LOX-1 on EPA and DHA regarding the immune system. Immune cells play critical roles in CRC and CAC (49). Omega-3 PUFAs are emerging as potent immune-regulators in CRC and CAC (50). In a double-blind clinical trial with breast cancer patients fed with EPA and DHA enriched fish oils, $CD4^+$ levels remained stable and suggesting beneficial immune response (51). An in vitro study showed EPA reducing indoleamine 2,3-dioxygenase 1 (IDO) levels, an important proponent in tumor immune escape by reducing T cell proliferation and survival (52).

The current study examines the role of 15-LOX-1 as a host factor in modulating the effects of DHA on the immune response to colitis, and EPA and DHA on tumorigenesis. We hypothesize that 15-LOX-1 expression in colonic epithelial cells is essential for resolvin E-series and D-series biosynthesis from EPA and DHA to alter immune cell polarization, limit inflammation, promote resolution, and ultimately help prevent colitis and CAC. Findings of this study could provide important information to aid future chemopreventive strategy development with these fish oil products and have immediate clinical relevance for individuals who are consuming DHA and EPA as dietary supplements.

2. Materials and Methods

2.1. Genetic mouse models

Mouse care and experimental protocol were approved and conducted in accordance with the guidelines of the Animal Care and Use Committee of the University of Texas MD Anderson Cancer Center. We have generated a novel mouse model with targeted humanized 15-lipoxygenase-1 (15-LOX-1) induced overexpression in colonic epithelial cells via a Rosa26 or

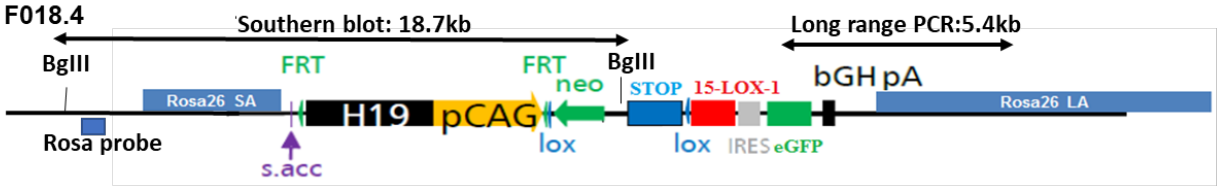

Figure 1. The strategy for generating a new inducible 15-LOX-1 mouse model (i15-LOX-1). The diagram of the vector (F018.4) design. For inducible overexpression of 15-LOX-1, two mouse models can be generated from one construct, the first (as shown) allowing inducible expression from the CAG promoter, the second from the mouse Rosa26 promoter. The genuine Rosa26 promoter is further upstream, and once in embryonic stem (ES) cells, its transcript is spliced into the splice acceptor of exon 2 ("s.acc.", purple). In the native state, transcription is aborted at the insulator site (H19, black), and instead starts at the CAG promoter (pCAG, yellow arrow). The loxP-flanked (lox, blue arrow heads) neo–STOP cassette for conditional activation has a stop site that is a large region of the SV40 intron plus late polyA (neo, green arrow; STOP, blue box). The cDNA is inserted downstream of the neo/stop cassette and is followed by an IRES driven eGFP reporter gene. Both Rosa26-driven and CAG-driven expression is polyadenylated at a bovine growth hormone polyA site (bGH pA, small black box). For exchange of the promoters, the CAG-cassette is flanked by FRT-sites.

CAG promoter. The strategy for generating a new inducible 15-LOX-1 mouse model is shown in **Figure 1**. Two mouse models can be generated from one construct. In this work, we used the Rosa26 promoter-driven inducible 15-LOX-1 (designated at Rosa-i15-LOX-1) mice with a genetic C57/BL6 background, which conditionally overexpressed 15-LOX-1 by upstream loxP-flanked stop sites and followed by IRES driven eGFP reporter gene (**Figure 1)**. This novel Rosa-i15- LOX-1 mouse model was generated in collaboration with PolyGene Transgenetics (Switzerland). B6.Cg-Tg(CDX2-Cre)101Erf/J (designated as CDX2-Cre, Catalog # 009350) mice were purchased from Jackson Laboratory. CDX2-Cre mice specifically express Cre recombinase mainly in the epithelial lining of the intestine, especially the colon. Breeding Rosa-i15-LOX-1 mice with CDX2-Cre mice generated CDX2-Cre; Rosa-i15-LOX-1 (designated as CDX2-Cre/Rosa-i15-LOX-1) mice that removed the loxP flanked stop site upstream of the 15-LOX-1-IRES-GFP cassette to overexpress 15-LOX-1 in the mice colon. For this work, the breeding scheme generated CDX-Cre/Rosa-i15-LOX-1 mice and CDX2-Cre/WT mice.

2.2. Mouse Genotyping

Genomic DNA was extracted from mouse ear snips using the method as follows: 1) mouse ear (around 3×3 mm) per mouse was cut and then digested in 250µl 0.05M sodium hydroxide at 95 °C heat block for 30 minutes; 2) after cool down, 25µl of 1M Tris pH 8.0 with 10mM EDTA buffer was added in the digested sample; and 3) the sample was vortexed and centrifuged at 12000 rpm for 10 minutes. The supernatant of the sample was used for mouse genotyping. The mice genotyping was performed by measuring genomic 15-LOX-1 coding sequence with qPCR method using around 10ng genomic DNA in 10µl reaction. Mouse actin was also measured at the same time by qPCR to exclude the possibility of false negatives. 15-LOX-1 and actin probes for qPCR were purchased from Integrated DNA Technologies (IDT, Catalog # Hs.PT.51.21032869 for human 15-LOX-1 and Catalog # Mm.PT.51.9990212 for mouse actin). 2×Master Mix, ABI Prism TM (Catalog # KK4707) was purchased from Kapa Biosystems.

2.3. Treatment and Induction of Colitis in Mice

CDX2-Cre/WT (WT) and CDX-Cre/Rosa-i15-LOX-1 (15-LOX-1) mice were randomly assigned to the control diet (Envigo; Teklad Custom Diet Diets, Catalog # TD.120422), or the control diet supplemented with 1% ethyl ester DHA (EE-DHA, Envigo; Teklad Custom Diet, Catalog # TD.160450). Pure EE-DHA was purchased from NU-CHEK PREP INC (Catalog # U-84E). Feeding started 8 weeks prior to colitis induction and continued until they were euthanized. Diet was stored at 4°C in sealed bags and replaced every other day to ensure quality and prevent autooxidation. Body weight was measured weekly.

For induction of colitis, mice 27 weeks of age received 3.0% dextran sodium sulfate (DSS) (molecular weight, 36,000–50,000; MP Biomedicals, Santa Ana, CA, USA) in drinking water for 7 days, followed by regular drinking water until sacrificed. For the acute colitis experiment, mice were sacrificed at peak inflammation, 1 day after the completion of DSS or when the mice developed sufficient morbidity to require euthanasia (n = 5-7 per group). For the chronic colitis experiment, mice were sacrificed 21 days after the completion of DSS to allow for chronic colitis development or when the mice developed sufficient morbidity to require euthanasia (n = 5-7 per group). Then the mice were killed, and colon tissue from each mouse was used for RNA, protein, immunohistochemistry staining, and flow cytometry immune cell profiling analyses. As shown in **Figure 2**, DSS was properly administered and caused body weight loss, a standard indicator for effective colitis induction. For the chronic colitis experiment, body weights also showed sufficient time allotted for full or partial resolution. Anal bleeding and stool consistency grades were also assessed (data not shown).

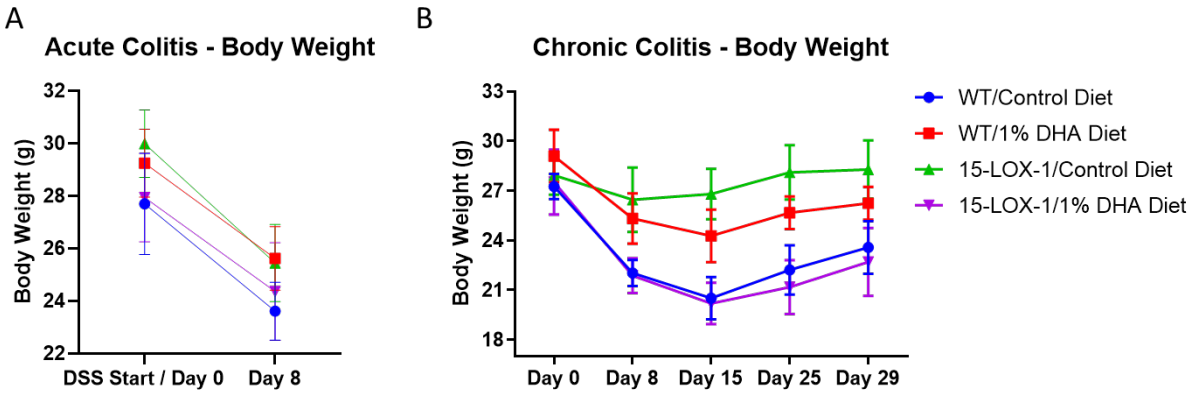

Figure 2. Effects of dextran sulfate sodium (DSS) induced colitis on body weight. Average body weight for the acute (A) and chronic (B) mouse groups. The data shown in panels A and B are means ± standard error of the mean (SEM).

2.4. Treatment and Induction of CAC in Mice

CDX2-Cre/WT (WT) and CDX-Cre/Rosa-i15-LOX-1 (15-LOX-1) were randomly assigned to the control diet (Envigo; Teklad Custom Diet Diets, Catalog # TD.120422), or the control diet supplemented with 1% EE-DHA or supplemented with 1% EE-EPA (Envigo;

Teklad Custom Diet, Catalog # TD.160450 for 1% EE-DHA diet or Catalog # TD.160449 for 1% EE-EPA diet). Pure EE-EPA was a free gift from S.L.A. Pharma INC. Differentials feeding started at 8-10 weeks of age and continued until they were euthanized. Diet was stored at 4°C in sealed bags and replaced every other day to ensure quality and prevent autoxidation. Body weight was measured weekly. The following models are based on a previous study by our group to induce CAC in mice (48).

For induction of CAC in mice fed with 1% EE-DHA, mice 12–14 weeks of age were injected intraperitoneally with azoxymethane in saline solution (AOM, Catalog # A5486, Sigma-Aldrich, St. Louis, MO, USA) at 10.0mg/kg. The mice received 3 cycles of 1.2% DSS in drinking water for 7 days, followed by 14 days of regular drinking water with the last cycle of DSS followed by 25 days of regular drinking water (n = 15 mice per group). The mice were killed approximately 13 weeks after AOM injection or when the mice developed sufficient morbidity to require euthanasia. The entire intestinal tract was removed, washed in cold PBS, and processed to assess for tumor burden as previously described (47). Colon tissue from each mouse was used for RNA, protein, immunohistochemistry staining, and eicosanoid and resolvin profiling analyses.

For induction of CAC in mice fed with 1% EE-EPA, mice 12–14 weeks of age were injected intraperitoneally with AOM at 10.0mg/kg. The mice received 3 cycles of 1.2% DSS in drinking water for 5 days, followed by 16 days of regular drinking water with the last cycle of DSS followed by 25 days of regular drinking water (n = 11-16 mice per group). The mice were killed approximately 13 weeks after AOM injection or when the mice developed sufficient morbidity to require euthanasia. The entire intestinal tract was removed, washed in cold PBS, and processed to assess for tumor burden as previously described (47). Colon tissue from each mouse was used for RNA, protein, and immunohistochemistry staining analyses.

2.5. Isolation of Lamina Propria Cells

Colon lamina propria cells were isolated as previously described with modifications (53). The colon was carefully separated from the cecum and Peyer's patches were removed. The colon was opened longitudinally, washed in cold PBS, and cut into 1 cm pieces. Epithelial cells were separated from the underlying lamina propria by incubation in HBSS containing 5mM EDTA and 2mM DTT for 20 minutes at 37°C with gentle rotation in a water bath shaker (150 rpm). Cells were removed using 10% FBS in RPMI through a 100μm strainer. Epithelial cell separation was repeated two times. Lamina propria tissue was pulse-vortexed and washed two times in PBS. The remaining tissue was finely chopped with a razor blade and digested in a solution of 200μg/mL Collagenase type VIII (Catalog # C2139, Sigma-Aldrich), 150μg/mL DNase I (Catalog # DN25, Sigma-Aldrich), and 25μg/mL Dispase in serum-free RPMI. Digestion solution with tissue was vortexed intensely for 20 sec then incubated for 20 min at 37°C with gentle rotation in a water bath shaker (150 rpm). Digested tissue was collected with a 40μm strainer. Tissue digestion was repeated two times or until connective tissue was no longer visible. Leukocytes were isolated from the supernatant using a Percoll (Catalog # 17089101, GE Healthcare Life Sciences) gradient separation method in which the cells were resuspended in 40% Percoll and under layered with 80% Percoll followed by centrifugation at 1000g or ~3000 RPM for 20 min at 20°C without brake. The interface was collected to wash with PBS and resuspended for red blood cell lysis (Catalog # 420301, Biolegend). Cells were resuspended in cell staining buffer (Catalog # 420201, Biolegend) for flow cytometry analysis. Cells numbers were determined using a Bright-Line Hemacytometer (Hausser Scientific) to have at least 1.0 E6 cells/mL per tube for staining.

2.6. Antibodies and Flow Cytometry

Lymphocytes extracted from the colon lamina propria were used for staining. I-A/I-E-PE (M5/114.15.2, Catalog # 107607), CD45-PerCP/Cy5.5 (30-F11, Catalog # 103131), CD49b-PE/Dazzle 594 (DX5, Catalog # 108923), CD11b-PE/Cy7 (M1/70, Catalog # 101215), CD4-FITC (GK1.5, Catalog # 100405), CD25-BUV785 (PC61, Catalog # 102051), CD11c-BUV711 (N418, Catalog # 117349), CD3-BUV650 (17A2, Catalog # 100229), Ly-6C-BUV510 (HK1.4, Catalog # 128033), F4/80-BUV421 (BM8, Catalog # 123131), Ly-6G-APC/Fire 750 (1A8, Catalog # 127651), and CD45R/B220-AF700 (RA3-6B2, Catalog # 103231) were purchased from Biolegend; CD8a-BUV737 (53-6.7, Catalog # 564297) was purchased from BD Biosciences to use in extracellular staining. If cells were to be analyzed the next day, they were fixed in a fixation buffer (Catalog # 420801, Biolegend). Intracellular mouse staining was performed according to the manufacturer's protocol (True Nuclear Transcription Factor Buffer Kit, Catalog # 424401; Biolegend) with FoxP3-AF647 (MF-14; Catalog # 126407, Biolegend). Fc receptors were blocked according to the manufacturer's protocol (TruStain fcX (93); Catalog # 101319, Biolegend). Dead cells were excluded using the Zombie UV fixable viability kit (Catalog # 423107, Biolegend). Respective UltraComp eBeads compensation beads were purchased from Thermo Fisher (Catalog # 01-2222).

The single 15-color flow cytometry panel and analysis were performed with a LSRFortessa X-20 (BD Biosciences) at the MD Anderson flow cytometry core facility and the data were analyzed using FlowJo software (Tree Star).

2.7. Mouse intestinal tumorigenesis evaluation

The mice were euthanized, the intestines from the rectum to the base of the cecum were removed, opened, washed with phosphate-buffered saline, and fixed with 10% neutral formalin

overnight. Tumors were counted under a stereotype microscope (Nikon SMZ1000). The colons were rolled up using a paper clip with a small loop to make Swiss rolls. The rolls were cut in half and placed in a paraffin cassette for embedding in paraffin for further analysis such as immunohistochemistry staining (IHC), and hematoxylin and eosin staining (H&E). Classification and grading of H&E-stained sections were performed by an experienced lab member.

2.8. Colitis Scoring

H&E stained sections were examined microscopically as previously described (54). To evaluate the severity of inflammation, an experienced lab member blinded to the treatment protocol randomly selected and inspected 10 fields (magnification ×100) in each section, and graded as follows: grade 0, normal colonic mucosa; grade 1, loss of one-third of the crypts; grade 2, loss of two-thirds of the crypts; grade 3, lamina propria covered with a single layer of epithelial cells with mild inflammatory cell infiltration; and grade 4, erosions and marked inflammatory cell infiltration. After grading the 10 fields, the mean grade was calculated for each mouse section and expressed as a histological score.

2.9. Immunohistochemical Analysis

IHC was performed as described before (55, 56). Colon tissues from the indicated experimental mice were fixed in 10% buffered formalin, embedded in paraffin, and cut into 5μm sections. The tissue sections were deparaffinized and rehydrated and antigen retrieval was performed with antigen unmasking solution (Vector Laboratories). Then, the sections were incubated in blocking buffer (phosphate-buffered saline with 1.5% goat serum and 0.3% Triton X-100) for 1 hour at room temperature and incubated with primary antibodies in a humidified

chamber at 4°C overnight. For IHC, the following primary antibodies were used: F4/80 (1:250; Catalog # 70076S, Cell Signaling); and Ki67 (1:300; Catalog # RM-9106-S1, Invitrogen, Carlsbad, CA). Subsequently, the tissue sections were incubated with biotinylated secondary antibodies (VECTASTAIN ABC kit; Vector Laboratories) for 1 hour, followed by incubation with avidin-coupled peroxidase (Vector Laboratories) for 30 minutes. 3, 3'-diaminobenzidine (DAB; Agilent Dako) was used as the chromogen, and the slides were counterstained with Mayer's hematoxylin (Agilent Dako).

2.10. Macrophage Quantification

F4/80 stained sections were examined microscopically. To evaluate the number of macrophages, an experienced lab member blinded to the treatment protocol randomly selected and inspected 10 fields (magnification ×100) in each section, and graded them as follows: grade 0 – 0% stained cells; grade 1 – 1-25% stained cells; grade 2 – 25-50% stained cells; grade 3 – 50-75% stained cells; and grade 4 – over 75% stained cells. The percentages refer to the ratio of positive signal (brown) to total signal (brown plus hematoxylin blue) per field. After grading the 10 fields, the mean grade was calculated for each section and expressed as a histological score.

2.11. Proliferation Quantification

Ki67 stained sections were examined microscopically. To evaluate the proliferation zone length, an experienced lab member blinded to the treatment protocol randomly selected and inspected 10 fields (magnification ×100) in each section, and measured the length of consecutive Ki67 positive cells in the colonic crypts. After grading the 10 fields, the mean grade was calculated for each section and expressed as a proliferation zone length (μm) per mouse.

2.12. Eicosanoid and Resolvin Profiling Analysis

Liquid Chromatography-Mass Spectrometry (LC-MS/MS) analyses were performed using an Agilent 6460 Triple Quad mass spectrometer (Santa Clara, CA) equipped with an Agilent 1200 HPLC as previously described (57-59). Eicosanoids were separated using a Kinetex C18 2.0×100 mm column (Phenomenex, Torrance, CA). The mobile phase consisted of 0.1% formic acid in water (A) and 0.1% formic acid in acetonitrile (B). For the analysis of PGE2, LXA4, LXB4, 15-HETE, and 13-HODE, the separation was achieved using a linear gradient of 20–98% of B with a total time of 33 min. The flow rate was 400µL/min with a column temperature of 30°C. The sample injection volume was 15µL. Samples were kept at 4 °C during the analysis. The mass spectrometer was operated in the electrospray negative ion mode with a gas temperature of 350°C, gas flow rate of 10L/min, and nebulizer pressure of 30psi. The temperature of the sheath gas was 350°C and sheath gas flow rate was 12L/min. The capillary voltage was -3500V. Fragmentation for all compounds was performed using nitrogen as the collision gas. All eicosanoids were detected using electrospray negative ionization and multiple-reaction monitoring (MRM) mode. The MRM transition for PGE2 was m/z 351.2→271.2, LXA4 was m/z 351.2→115.2, LXB4 was m/z 351.2→221.1, 15-HETE was m/z 319.2→219.2, and 13-HODE was m/z 295.2→195.2. The results were expressed as nanograms of eicosanoid per mg of protein.

Resolvins were separated using an Agilent XDB C18 4.6×50mm column. The mobile phase consisted of 10mM ammonium acetate in water (A) and methanol (B). For the analysis of RVD1, RVD2, RVD3, RVD4, RVD5, RVE1, 17-HDHA and 18-HEPE, the separation was achieved using a linear gradient of 20–90% of B with a total time of 20 min. The flow rate was 300µL/min with a column temperature of 30°C. The sample injection volume was 15µL. Samples were kept at 4°C during the analysis. The mass spectrometer was operated in the

electrospray negative ion mode with a gas temperature of 350°C, gas flow rate of 10L/min, and nebulizer pressure of 20psi,, The temperature of the sheath gas was 350°C and sheath gas flow rate was 12L/min. The capillary voltage was -2900V. Fragmentation for all compounds was performed using nitrogen as the collision gas. All resolvins were detected using electrospray negative ionization and MRM mode. The MRM transition for RVD1 was m/z 375.1→215.1, RVD2 was m/z 375.2→174.9, RVD3 was m/z 375.0→147.0, RVD4 was m/z 375.0→101.0, RVD5 was m/z 359.0→199.0, and 17-HDHA was m/z 341.3→201.1. The results were expressed as nanograms of resolvin per mg of protein.

2.13. Statistical Analysis

Two-way ANOVA analysis of variance was used to analyze data involving the simultaneous consideration of two factors. All tests were 2-sided and conducted at a significance level of $P < 0.05$. The data are presented as means ± standard error of the mean (SEM) and analyzed using Prism 9.0 software (GraphPad Software). The significance of correlation between DHA products and total tumor number per mouse was assessed by Spearman correlation coefficient test using SAS software, version 9.4 (SAS Institute).

3. Results

3.1. Characterization of the Novel Rosa-i15-LOX-1 Mouse Model

We first characterized the novel Rosa-i15-LOX-1 mice by breeding them with CDX-Cre mice to produce Rosa-i15-LOX-1/CDX2-cre (15-LOX-1) mice. Colon crypts were scraped from the indicated mice for 15-LOX-1 expression measurement by Western blot and 15-LOX-1's enzymatic products 13-HODE and 15-HETE levels by LC-MS/MS measurement. We found that 15-LOX-1 mice, but not the mice with other genotypes as indicated, expressed 15-LOX-1

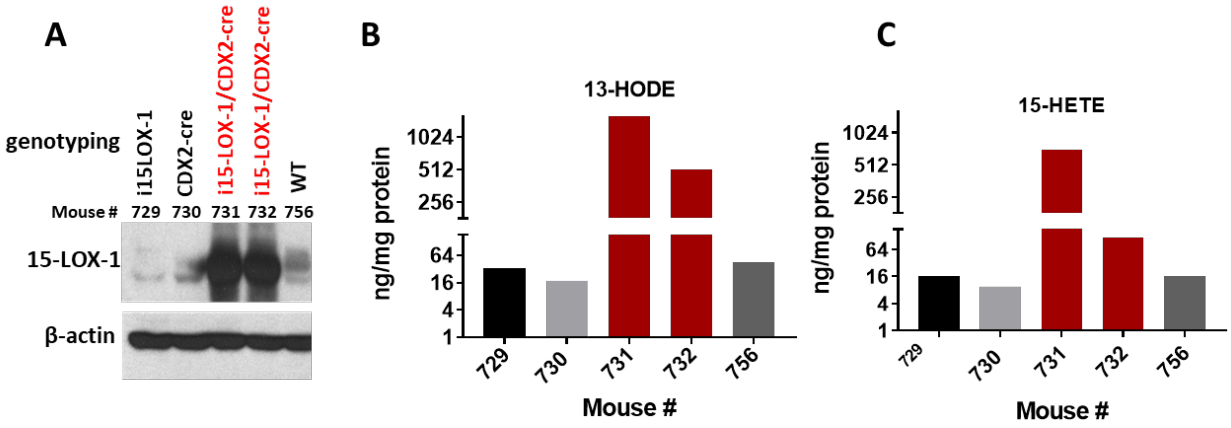

Figure 3. Characterization of the new Rosa-i15-LOX-1 mouse model. Rosa-i15-LOX-1 mice were bred with CDX-Cre recombinase mice to induce 15-LOX-1 overexpression in colon epithelial cells via targeted intestinal cre-recombinase expression driven by CDX2 promoter (CDX2-cre). Mice were euthanized, and colonic epithelial crypts were processed for 15-LOX-1 protein expression (Western blotting) and measurement of 15-LOX-1 products (13-HODE and 15-HETE) by LC-MS/MS. (A) Colonic 15-LOX-1 expression was induced in mice that expressed Cre-recombinase (731 and 732), but not in those that expressed i15-LOX-1 without Cre-recombinase (729), wild-type littermates (WT, 756), or those that expressed cre-recombinase alone (730). Colonic 15-LOX-1 expression was enzymatically active as demonstrated by markedly increased 13-HODE (B) and 15-HETE (C) levels.

(**Figure 3A**) and produced higher levels of 13-HODE and 15-HETE in colon epithelial cells (**Figure 3B and C**). Our results indicated that Rosa-i15-LOX-1 was successfully generated.

3.2. Effects of 15-LOX-1 and DHA on Acute and Chronic Colitis

In the acute DSS-induced colitis experiments, decreasing inflammation trends were observed in all experimental groups compared to the WT/Control diet groups, but no statistical significance was found between any of the groups (**Figure 4A**).

In the chronic DSS-induced colitis experiments (**Figure 4B**), we found that experimental 15-LOX-

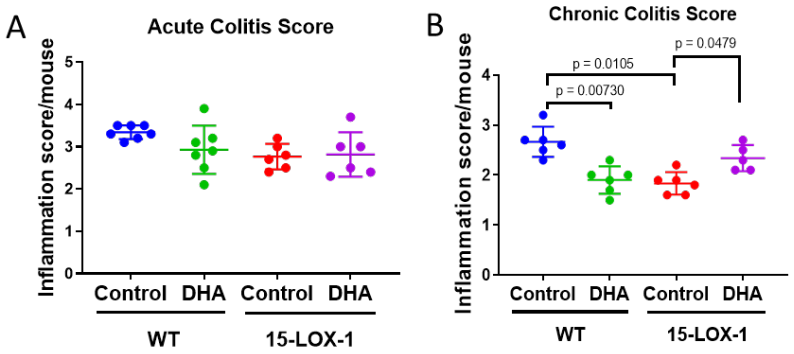

Figure 4. Effects of 15-LOX-1 modulation of docosahexaenoic acid (DHA) on dextran sulfate sodium (DSS) induced colitis. Average colitis scores for the acute (A) and chronic (B) mouse groups. The data shown in panels A and B are means ± standard error of the mean (SEM). P-values by 2-way ANOVA.

1/Control diet mice group (1.8 ± 0.092, p = 0.0105) reduced their inflammation scores by 31% and that WT/DHA mice group (1.9 ± 0.011, p = 0.0730) improved their inflammation scores by 29%, compared to the WT/Control diet mice group (2.7 ± 0.12). In addition, 15-LOX-1/Control diet mice significantly reduced inflammation, compared to the WT/DHA mice group (2.3 ± 0.12; p = 0.0246). Our results suggested that 15-LOX-1 and DHA alone significantly inhibited DSS-induced chronic colitis but had no significant effect on DSS-induced acute colitis. Unexpectedly, we did not observe an additive effect in mice with 15-LOX-1 and fed with DHA.

3.3. Effects of 15-LOX-1 and DHA on Immune Cells

A 15-color flow cytometry panel was designed to analyze immune cell subsets and characterize immunophenotype modulation in acute and chronic colitis experiments (**Table 1**). Colon samples with the same genotype were randomly pooled to 3 samples (2-3 colons/sample) per group for acute colitis and 1-2 samples (2-3 colons/sample) per group for chronic colitis before flow cytometry analysis.

Table 1. Immunophenotyping of mouse immune subsets by flow cytometry.

Immune cell subset	**Phenotype**
Macrophage	$CD11b^{+}F4/80^{+}$
Neutrophil	$CD11b^{+}Ly6G^{+}Ly6C^{lo}$
Monocyte	$CD11b^{+}Ly6G^{-}Ly6C^{hi}$
Helper T cell	$CD3^{+}CD4^{+}$
Regulatory T cell	$CD3^{+}CD4^{+}CD25^{+}Foxp3^{+}$
Cytotoxic T cell	$CD3^{+}CD8^{+}$
B cells	$B220^{+}$

Plasmacytoid Dendritic Cell (pDC)	$CD11c^{+}B220^{+}$
Conventional Dendritic Cell 1 (cDC1)	$CD11c^{+}CD8^{+}$
Conventional Dendritic Cell 2 (cDC2)	$CD11c^{+}CD4^{+}CD11b^{hi}$
Hematopoietic cell	$CD45^{+}$
Live/Dead	Viability

Note: Hematopoietic cells were initially counted from all detected cells using single cells, live cells, and $CD45^{+}$ gates. From the hematopoietic subset, $CD11b^{+}$ were gated to subsequently gate for monocytes, macrophages, neutrophils, and MDSCs. From the hematopoietic subset, $CD11c^{+}$ were gated to subsequently gate for dendritic cells. From the hematopoietic subset, $CD11b^{-}/c^{-}$ were gated to subsequently gate for T cells and B cells.

An immunophenotype modulating the immune system was examined in the acute colitis experiments (**Figure 5**). Some immune cells showed changes, but without statistical significances. In the innate cell populations, large standard errors within groups confounded detecting potential changes in the acute colitis immune cell profile. The monocyte population showed an increase in the 15-LOX-1/Control diet mice group and decrease in the 15-LOX-1/DHA mice group. However, there were no statistical significances to support the mentioned differences (**Figure 5**).

As expected, the adaptive immune system showed little change except for cDC2. In the 15-LOX-1/DHA mice group, we can see cDC2 increased compared to the other groups. Within the higher levels of helper T cells in the 15-LOX-1/Control diet mice group, we observe a lower number of regulatory T cells, though without statistical significance.

In the chronic colitis experiment, the chronic colitis experiments showed more differential results among immune cell populations (**Figure 6**). In the innate cells, high neutrophil count was sustained in the WT/DHA mice group, while the other groups remained

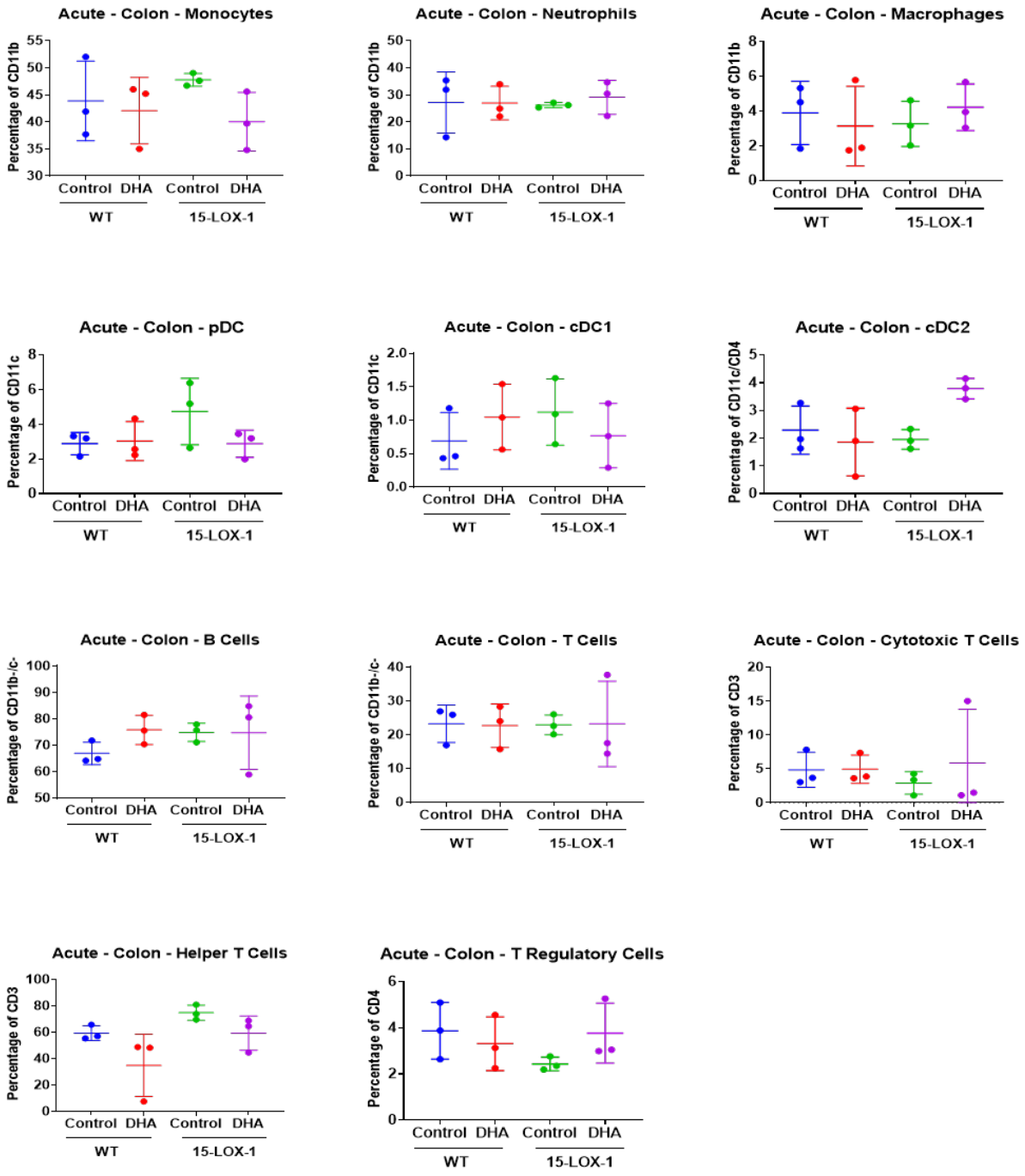

Figure 5. Immune profile of DSS-induced acute colitis. The WT mice fed with control diet is signified as WT/Control diet. The WT mice fed with DHA is signified as WT/DHA. The 15-LOX-1 mice fed with control diet is signified as 15-LOX-1/Control diet. Finally, the 15-LOX-1 mice fed with DHA is signified as 15-LOX-1/DHA. The data shown are means ± standard error of the mean (SEM).

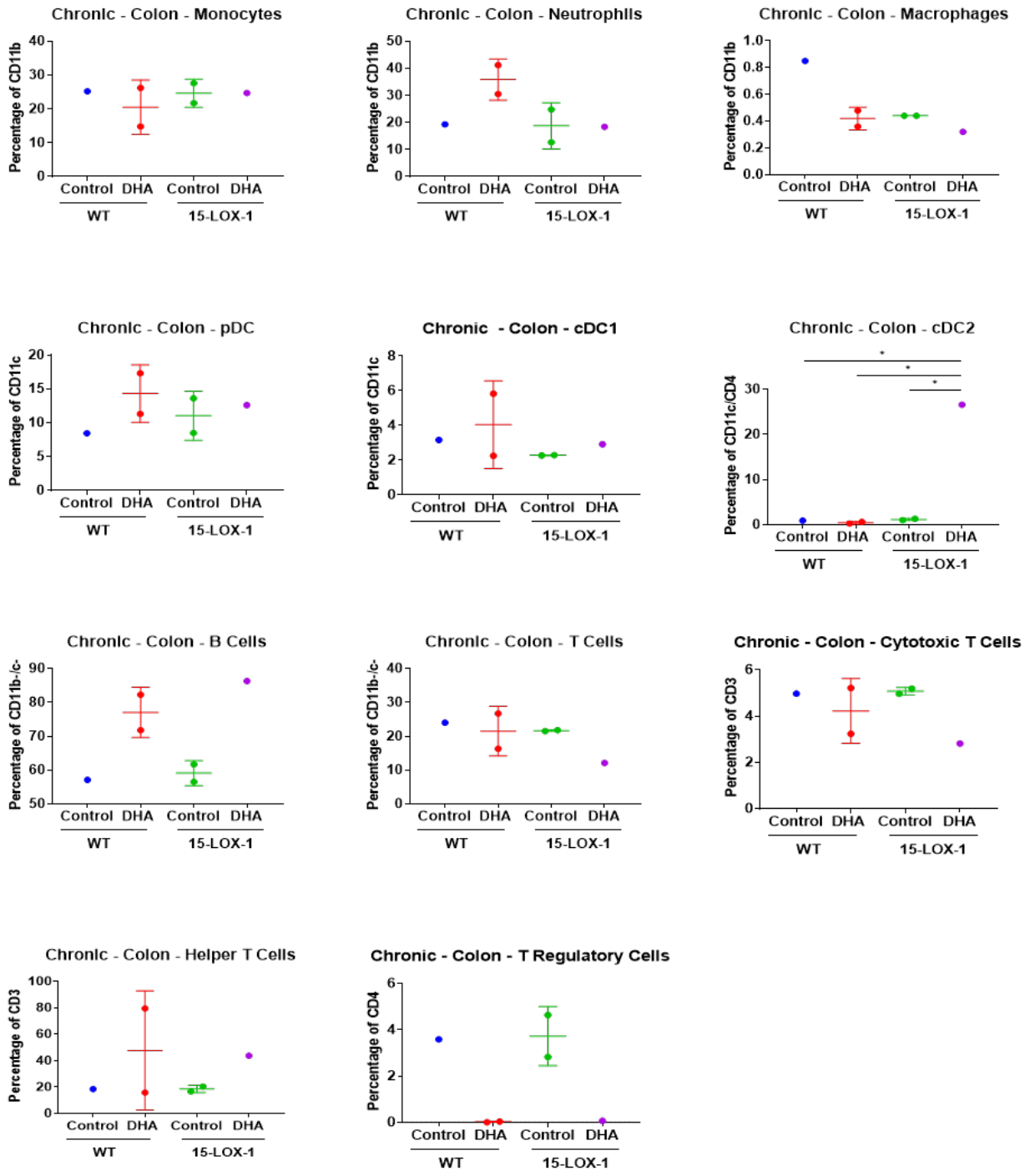

Figure 6. Immune profile of DSS induced chronic colitis. The WT mice fed with control diet is signified as WT/Control diet. The WT mice fed with DHA is signified as WT/DHA. The 15-LOX-1 group fed with control diet is signified as 15-LOX-1/Control diet. Finally, the 15-LOX-1 mice fed with DHA is signified as 15-LOX-1/DHA. The data shown are means ± standard error of the mean (SEM). * signifies $p < 0.0001$. P-values by 2-way ANOVA.

comparable to the WT/Control diet mice group. Macrophage counts were lower in all groups, with the lowest in the 15-LOX-1/DHA mice group. The monocyte populations showed lower levels in the WT/DHA and 15-LOX-1/DHA mice groups, while the 15-LOX-1/Control diet mice group remained high and comparable to the WT/Control diet mice group.

As expected in chronic inflammation, more differences were observed in the adaptive immune system. In the cDC2 population, the 15-LOX-1/DHA mice group was the only group that sustained high levels while the other groups showed levels close to negligible ($p < 0.0001$). The B cell population showed higher and comparable levels in the WT/DHA and 15-LOX-1/DHA mice groups compared to the WT/Control diet and 15-LOX-1/Control diet mice groups. T cells were shown to be decreased in only the 15-LOX-1/DHA mice group. Within this group, T helper cell counts were higher in the WT/DHA and 15-LOX-1/DHA mice groups. T regulatory cells were negligible in the WT/DHA and 15-LOX-1/DHA mice groups compared to the WT/Control diet mice group, while the 15-LOX-1/Control diet mice group showed comparable levels to the WT/Control diet mice group. Cytotoxic T cells remained at comparable levels to the WT/Control diet mice group except for the 15-LOX-1/DHA mice group, which showed lower levels (**Figure 6**). However, due to the small sample number limitations and large standard errors, all the results for chronic colitis are still preliminary. Nevertheless, even if definite conclusions cannot be drawn, the data could be indicative of changes. Future studies should include more samples per group, which might help find connections between immune cells changes and phenotypes.

3.4. Effects of 15-LOX-1 and DHA on CAC

Reduction in tumor numbers (mean ± SEM) was observed in both mice groups that were given DHA diet (WT/DHA and 15-LOX-1/DHA mice groups) compared to 8.6 ± 1.5

tumors/mouse in the WT/Control diet mice group (**Figure 7A and 7B**). A 54% reduction in tumor numbers occurred in the WT/DHA mice group (3.9 ± 0.97 tumors/mouse; p = 0.0348) and 52% reduction in the 15-LOX-1/DHA mice group (4.2 ± 0.90 tumors/mouse; p = 0.0479). In addition, we found that both 15-LOX-1 and DHA decreased large tumor numbers (tumor diameter >3mm) (**Figure 7C**).

Inflammation scores (mean ± SEM) showed improvement in all three experimental groups compared to the WT/Control diet mice group (2.3 ± 0.075) (**Figure 7D**). The 15-LOX-1/Control diet mice group reduced inflammation by 18% (1.9 ± 0.073; p < 0.0001), WT/DHA mice group by 33% (1.6 ± 0.13; p = 0.0362), and 15-LOX-1/DHA mice group by 29% (1.7 ± 0.13; p = 0.0015). Though we observed an 11% decrease in the 15-LOX-1/DHA and a 15%

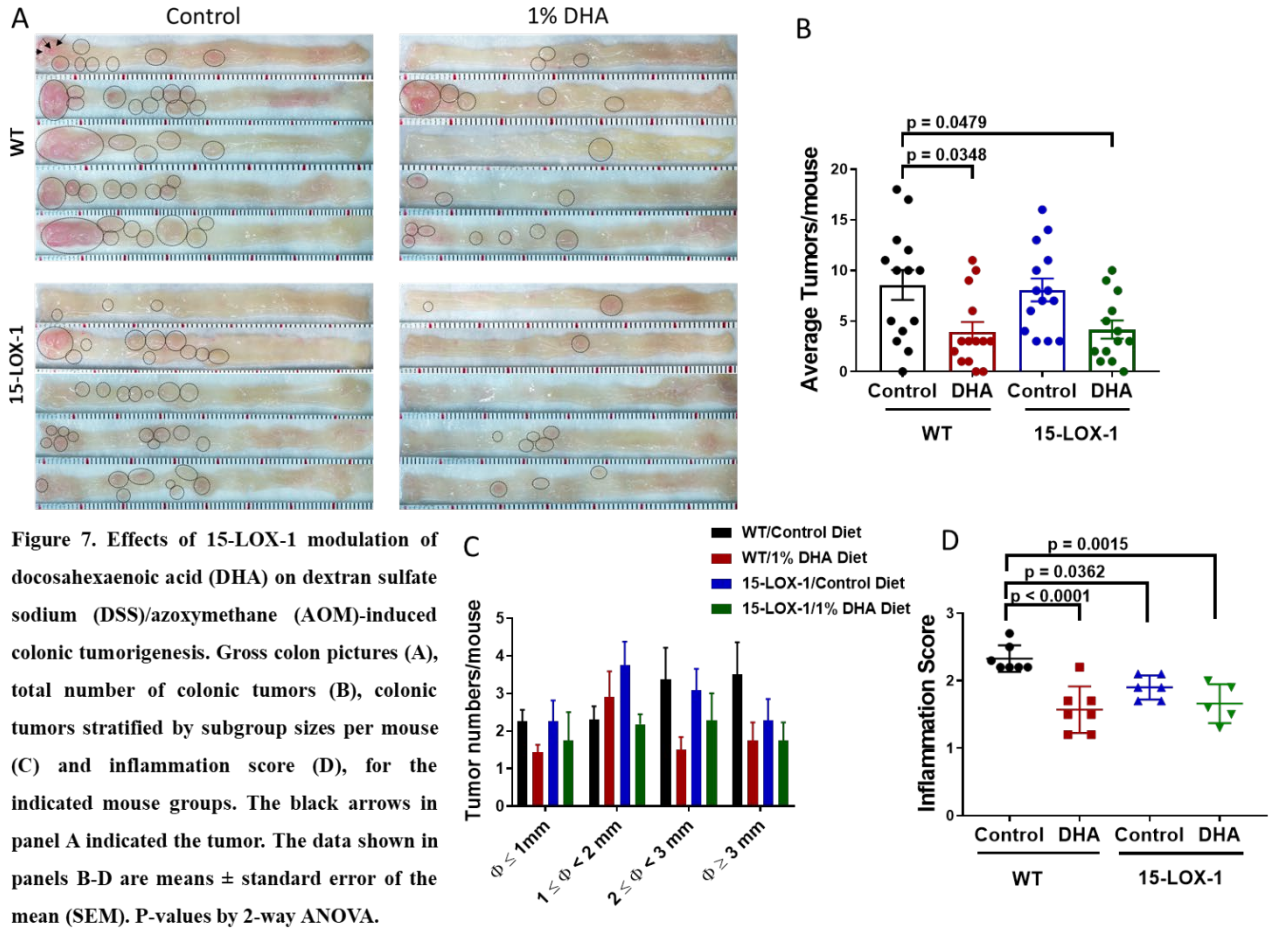

Figure 7. Effects of 15-LOX-1 modulation of docosahexaenoic acid (DHA) on dextran sulfate sodium (DSS)/azoxymethane (AOM)-induced colonic tumorigenesis. Gross colon pictures (A), total number of colonic tumors (B), colonic tumors stratified by subgroup sizes per mouse (C) and inflammation score (D), for the indicated mouse groups. The black arrows in panel A indicated the tumor. The data shown in panels B-D are means ± standard error of the mean (SEM). P-values by 2-way ANOVA.

decrease in the WT/DHA mice groups compared to the 15-LOX-1/Control diet mice group, there were no statistical differences.

3.5. Effects of 15-LOX-1 and DHA on Resolvin Production

Resolvin D-series and their precursor, 17-HDHA, were measured using LC-MS/MS analysis (mean ± SEM). All target products were dependent on mice having 15-LOX-1. Without 15-LOX-1, little to no resolvins were produced.

The precursor for resolvin D-series, 17-HDHA increased by a factor of 2.7 between the 15-LOX-1/Control diet (32.4 ± 3.66 ng/mg protein) and 15-LOX-1/DHA (87.6 ± 7.74 ng/mg

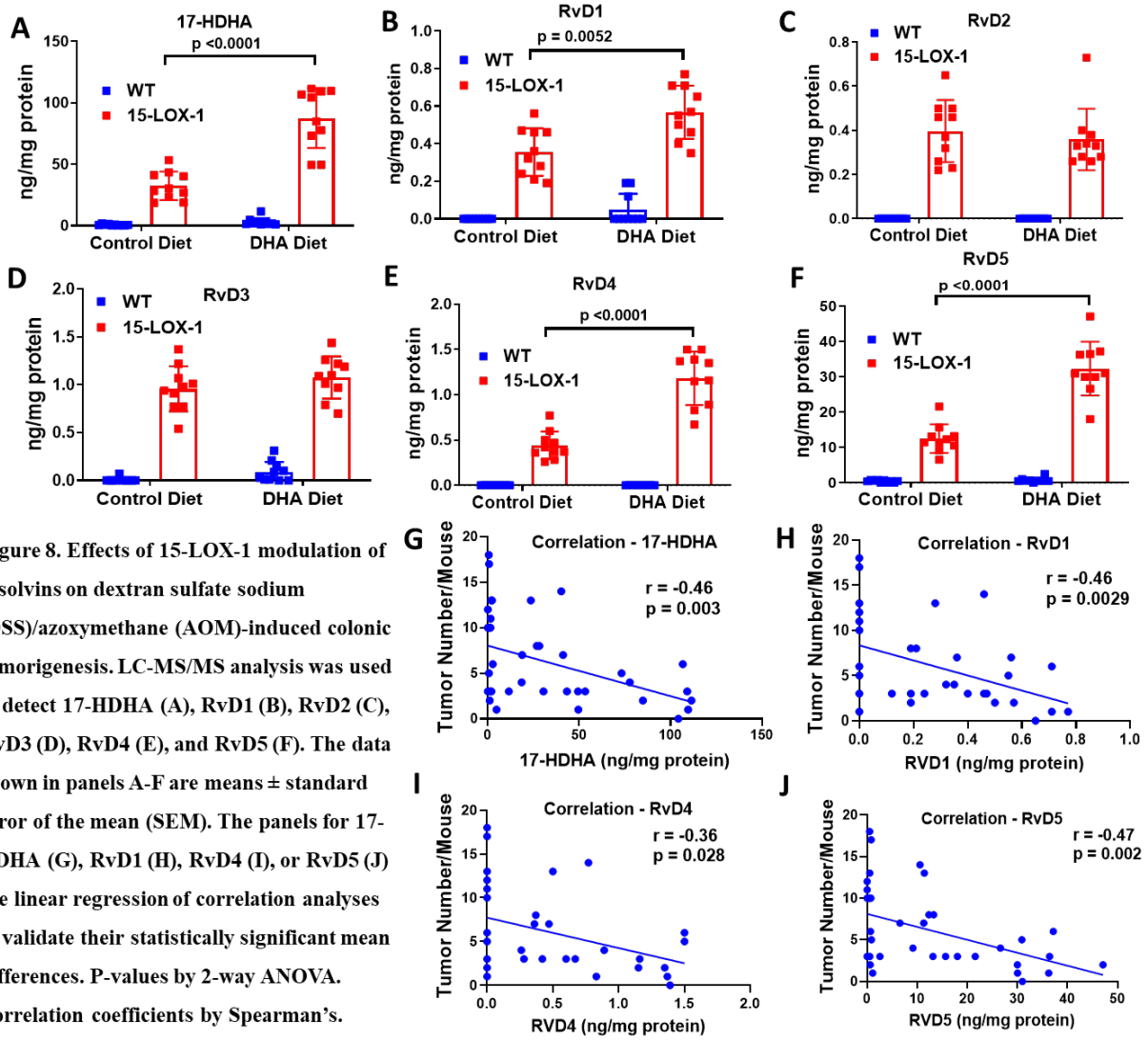

Figure 8. Effects of 15-LOX-1 modulation of resolvins on dextran sulfate sodium (DSS)/azoxymethane (AOM)-induced colonic tumorigenesis. LC-MS/MS analysis was used to detect 17-HDHA (A), RvD1 (B), RvD2 (C), RvD3 (D), RvD4 (E), and RvD5 (F). The data shown in panels A-F are means ± standard error of the mean (SEM). The panels for 17-HDHA (G), RvD1 (H), RvD4 (I), or RvD5 (J) are linear regression of correlation analyses to validate their statistically significant mean differences. P-values by 2-way ANOVA. Correlation coefficients by Spearman's.

protein) mice groups ($p < 0.0001$; **Figure 8A**). RvD1 (0.567 ± 0.045 ng/mg protein; $p = 0.0052$; **Figure 8B**), RvD4 (1.18 ± 0.0932 ng/mg protein; $p < 0.0001$; **Figure 8E**), and RvD5 (32.4 ± 2.41 ng/mg protein; $p < 0.0001$; **Figure 8F**) showed significant increases in the 15-LOX-1/DHA mice group compared to 15-LOX-1/Control diet mice group. More specifically, RvD1 increased by a factor of 1.6, RvD4 increased by a factor of 2.7, and RvD5 increased by a factor of 2.6. However, there was no significant difference for RvD2 and RvD3 between the 15-LOX-1 mice groups fed with control or DHA diets.

Correlation analyses of total tumor number per mouse were performed on 17-HDHA and resolvins that showed the following Spearman correlation coefficients: 17-HDHA ($r = -0.46$; $p = 0.003$), RvD1 ($r = -0.46$; $p = 0.0029$), RvD4 ($r = -0.36$; $p = 0.028$), and RvD5 ($r = -0.47$; $p = 0.002$) demonstrating inverse linear regression of correlations with total tumors per mouse (**Figure 8G-J**).

3.6. Effects of 15-LOX-1 and DHA on Eicosanoid Products

Eicosanoid products were measured using LC-MS/MS analysis. No statistical significances were observed between any of the groups for PGE2, LXA4, or LXB4 (**Figure 9A-C**). In addition, their production was not dependent on 15-LOX-1 expression. Both 15-LOX-1 enzymatic products 13-HODE and 15-HETE productions were dependent on mice expressing 15-LOX-1 (**Figure 9D-E**). 13-HODE showed significant decrease by a factor of 1.7 between the 15-LOX-1/Control diet (309.6 ± 38.10 ng/mg protein) and 15-LOX-1/DHA mice groups (185.9 ± 17.45 ng/mg protein; $p = 0.0021$; **Figure 9D**). 15-HETE showed significant decrease by a factor of 4.8 between the 15-LOX-1/Control diet (446.4 ± 38.21 ng/mg protein) and 15-LOX-1/DHA mice groups (92.42 ± 11.75 ng/mg protein; $p < 0.0001$, **Figure 9E**).

Correlation analysis with total tumors per mouse was performed on 13-HODE and 15-HETE (**Figure 9F-G**). 13-HODE showed a stronger inverse correlation (r = -0.2200) than 15-HETE (r = -0.0403) with total tumors per mouse. However, they both did not reach statistical significance (p = 0.3888; p = 0.8792, respectively).

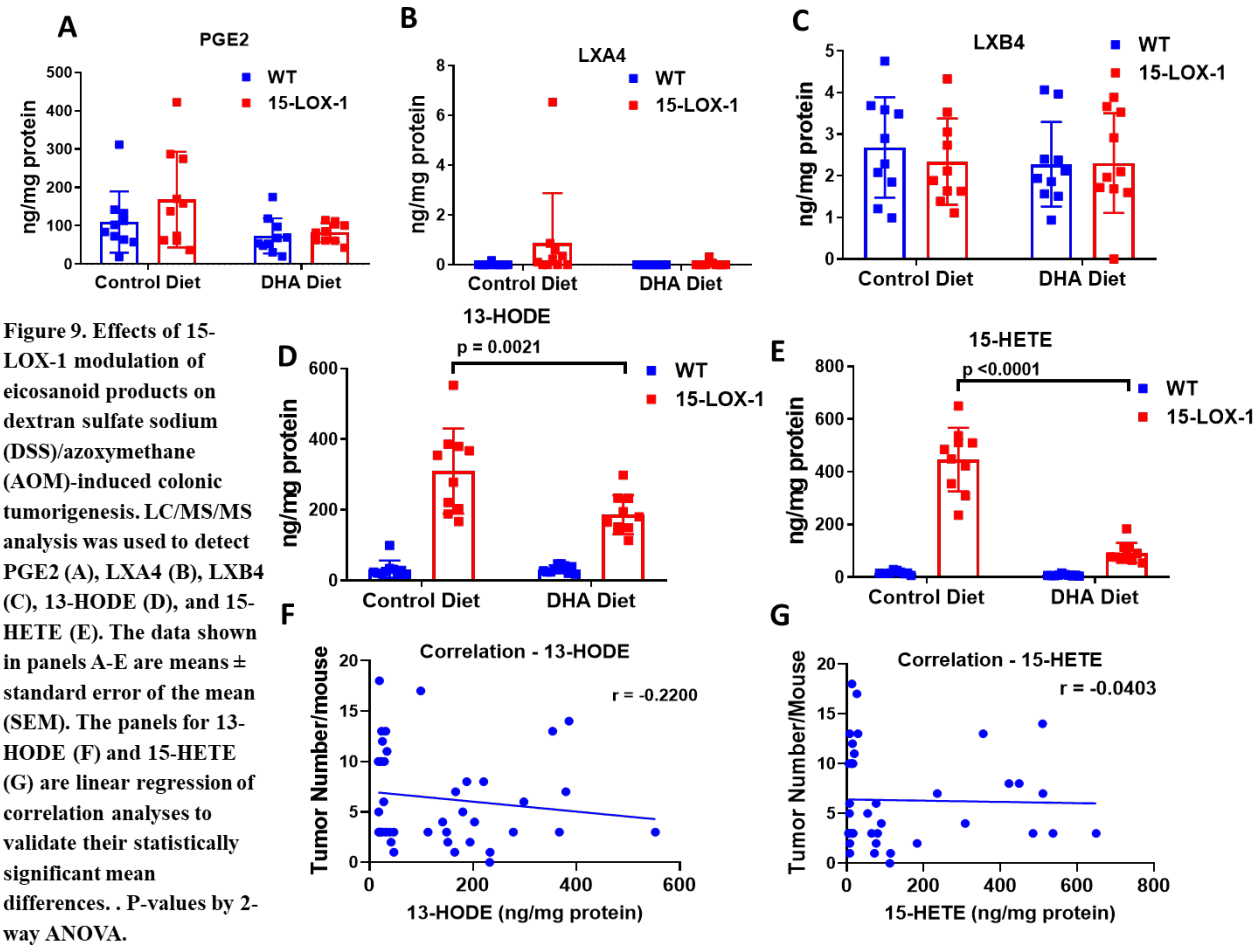

Figure 9. Effects of 15-LOX-1 modulation of eicosanoid products on dextran sulfate sodium (DSS)/azoxymethane (AOM)-induced colonic tumorigenesis. LC/MS/MS analysis was used to detect PGE2 (A), LXA4 (B), LXB4 (C), 13-HODE (D), and 15-HETE (E). The data shown in panels A-E are means ± standard error of the mean (SEM). The panels for 13-HODE (F) and 15-HETE (G) are linear regression of correlation analyses to validate their statistically significant mean differences. . P-values by 2-way ANOVA.

3.7. Effects of 15-LOX-1 and EPA on CAC

Tumor numbers (mean ± SEM) were significantly reduced in all experimental groups compared to the WT/Control diet mice group (**Figure 10A and B**). Compared to the WT/Control diet mice group (4.2 ± 0.98 tumors/mouse), tumors were reduced by 47% in the WT/EPA mice group (2.2 ± 0.66 tumors/mouse; p = 0.003), 48% in the 15-LOX-1/Control diet

mice group (2.2 ± 0.26 tumors/mouse; p = 0.004), and 48% in the 15-LOX-1/EPA mice group (2.2 ± 0.33 tumors/mouse).

Tumors categorized by size observed all groups reducing all tumor sizes but with the largest decrease in the larger tumors (**Figure 10C**). The 1 – 2 mm tumor incidence decreased in the WT/EPA mice group by 23% (1.4 ± 0.50 tumors/mouse), 15-LOX-1/Control diet mice group by 32% (1.3 ± 0.30 tumors/mouse), and 15-LOX-1/EPA mice group by 41% (1.1 ± 0.35 tumors/mouse), compared to the WT/Control diet mice group (1.9 ± 0.41 tumors/mouse). The 2 – 3 mm tumor incidence decreased in the WT/EPA mice group by 79% (0.1 ± 0.1 tumors/mouse), 15-LOX-1/Control diet mice group by 73% (0.2 ± 0.1 tumors/mouse),

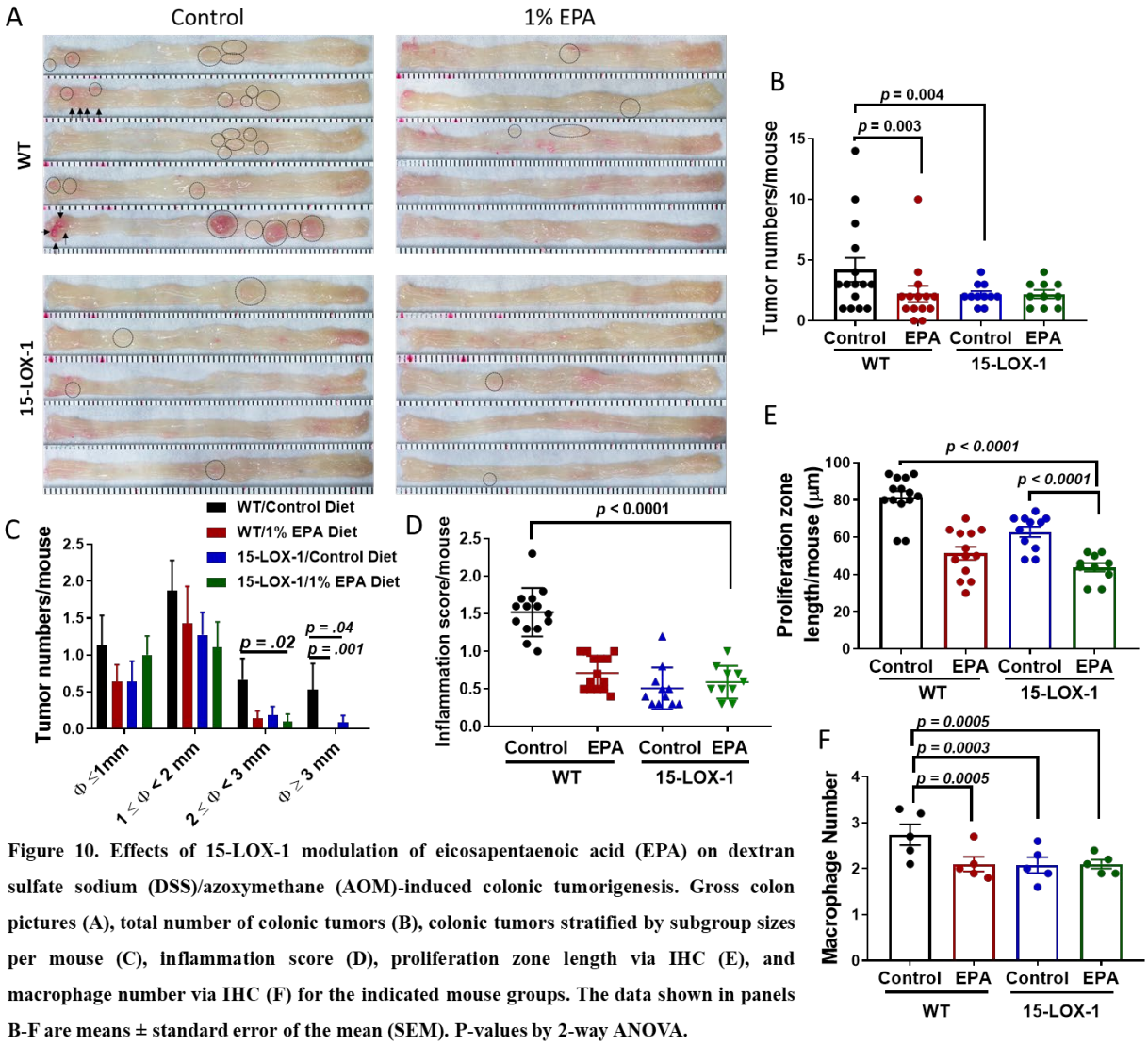

Figure 10. Effects of 15-LOX-1 modulation of eicosapentaenoic acid (EPA) on dextran sulfate sodium (DSS)/azoxymethane (AOM)-induced colonic tumorigenesis. Gross colon pictures (A), total number of colonic tumors (B), colonic tumors stratified by subgroup sizes per mouse (C), inflammation score (D), proliferation zone length via IHC (E), and macrophage number via IHC (F) for the indicated mouse groups. The data shown in panels B-F are means ± standard error of the mean (SEM). P-values by 2-way ANOVA.

and 15-LOX-1/EPA mice group by 85% (0.1 ± 0.1 tumors/mouse; $p = 0.02$), compared to the WT/Control diet mice group (0.7 ± 0.3 tumors/mouse). Large tumors (> 3 mm) were not observed in the WT/EPA mice group ($p = 0.001$) or the 15-LOX-1/EPA mice group, and minimally observed in 15-LOX-1/Control diet mice group (0.1 ± 0.1 tumors/mouse; $p = 0.04$), compared to the WT/Control diet mice group (0.5 ± 0.4 tumors/mouse).

Inflammation, proliferation zones, and macrophage number paralleled the tumor number trend. A decrease was observed in all experimental groups regarding inflammation score compared to WT/Control diet mice group (**Figure 10D**). Inflammation scores were reduced by 53% (0.7 ± 0.1) in the WT/EPA mice group, by 67% (0.5 ± 0.1) in the 15-LOX-1/Control diet mice group, and by 61% (0.6 ± 0.1; $p < 0.0001$) in the 15-LOX-1/EPA mice group, compared to the WT/Control diet group (1.5 ± 0.09).

As shown in **Figure 10E**, proliferation zones were measured to determine the growth capacity of crypts. Longer proliferations zones are associated larger growth capacity in crypts, which is a strong risk factor for tumorigenesis. Compared to the WT/Control diet mice group (81.7 ± 3.01 μm), the WT/EPA mice group reduced proliferation zone length by 37% (51.4 ± 3.52 μm), 15-LOX-1/Control diet mice group by 23% (62.9 ± 2.82 μm), and 15-LOX-1/EPA mice group by 46% (43.8 ± 2.30 μm; $p < 0.0001$). In addition, the 15-LOX-1/EPA mice group showed statistically significant reduction compared to the 15-LOX-1/Control diet ($p < 0.0001$) mice group.

In **Figure 10F**, compared to WT/Control diet mice group, all experimental groups demonstrated reduced macrophage numbers, but they were comparable to each other. The WT/EPA mice group was reduced by 23% (2.1 ± 0.16; $p = 0.0005$), 15-LOX-1/Control diet mice group by 24% (2.1 ± 0.17; $p = 0.0003$), and 15-LOX-1/EPA mice group by 23% (2.1 ± 0.095; $p = 0.0005$) compared to the control group (2.7 ± 0.23).

4. Discussion

We found evidence that EPA, DHA, and expression of human 15-LOX-1 in colonic epithelial cells modulates chronic colitis and colitis-associated colorectal tumorigenesis in mice. Studies of specific 15-LOX-1 functions in mouse models require transgenic expression of human 15-LOX-1 because the mouse homolog 12/15-LOX produces both 12-HETE and 13-HODE, which elicit opposing biological effects on tumorigenic processes (60, 61). It has also been shown to both inhibit (62) and activate TNF-α-iNOS signaling (63); possibly by 13-HODE (64) and 12-HETE (63), respectively. Together, highlighting the importance of determining the precise impact of human 15-LOX-1 expression in colonic epithelial cells.

In the acute colitis experiment, the lack of differentiated inflammation scores and immune cell profiles may be secondary to non-optimal DSS dosing, causing too much damage to the gut epithelial cells (**Figure 4A and 5**). Though some damage to the epithelial lining is necessary to induce colitis, a loss of epithelial cell function interrupts gut homeostasis (65). Nevertheless, we do see a consistent increase in cDC2 in the 15-LOX-1/DHA mice group. cDC2s secrete higher levels of IL-12, which increases bacterial antigen presentation to $CD8^+$ T cells, T helper type 1 cells, and natural killer cells (66). This mechanism is partially supported with some $CD8^+$ T cell samples increased in the 15-LOX-1/DHA mice group. DHA or 15-LOX-1 expression could not combat the strong physical disruption of DSS, but rather, contribute more so in the resolution phase of chronic colitis.

In the chronic colitis experiment, all experimental groups exhibited improved inflammation scores upon euthanasia. This can certainly be attributed to the 3 weeks given to mice for recovery mechanisms to elicit function. Unlike the acute experiments, we observe more differentiated inflammation scores and immune profiles (**Figure 4B and 6**). Interestingly, mice with 15-LOX-1 mice or WT mice fed with DHA reduced inflammation the most, while 15-

LOX-1/DHA did not improve inflammation scores as much. Improved inflammation from 15-LOX-1 expression supports findings from previous studies (27). Though we expected to observe an additive effect when combining 15-LOX-1 expression and DHA, data shows omega-3 PUFAs can be metabolized by several tissue types (67). Emerging evidence links interactions between 15-LOX-1 and tumor associated macrophages (TAMs) (27, 67). 15-LOX-1 expression can be induced in TAMs following engulfment of apoptotic cells and support anti-inflammation (68). This mechanism may explain how DHA without expression of the 15-LOX-1 transgene can still elicit an anti-inflammatory response. More importantly, the delicate balance between monocytes/macrophages and neutrophils can swing the immune cell profile into a potent anti-inflammation phenotype (69, 70). This phenotype is defined as low neutrophil levels, polarization to M2 macrophages, and high monocyte count. A critical aspect of the resolution phase is timely removal of neutrophils. Apoptosis or necrosis of neutrophils regulate TNF and nitric oxide production from monocyte-derived macrophages and increase their phagocytic index (71). This switch enhances efferocytosis and alters macrophages to "wound heal" by promoting matric deposition, tissue remodeling, and tissue repair (72). For this experiment, follow up experiments will use more markers to determine their M1 or M2 polarization. Neutrophils improve their anti-inflammatory function by recruiting high amounts of monocytes (73). Low amounts of monocyte recruitment worsened outcome in peritoneal bacteremia mice (74). 15-LOX-1 expression with control diet may have shown the largest improvement in inflammation by controlling the monocyte/macrophage and neutrophil balance.

In addition, the 15-LOX-1/Control diet mice group showed higher levels of T regulatory cells. Their immunosuppressive role are beneficial to inflammation as they prevent self-tolerance and excessive inflammation (75). Transfer of T regulatory cells has previously prevented development of colitis by reducing lamina propria infiltration and reappearance of

normal intestinal tissue (76). The 15-LOX-1/Control diet mice group also showed increased cytotoxic T cells. However, their exact function has not been determined as pro or anti-inflammatory cells. One study reported high levels of cytotoxic T cells associated with ulcerative colitis progression (77). In other studies, cytotoxic T cells with PD-1 expression prevent response to intestinal self-antigen (78, 79), alluding to a potential beneficial role in anti-inflammation.

Our study has provided a general image of how 15-LOX-1 modulates colitis through the immune system. Follow up functional studies on immune cells along with cytokine and marker analysis are necessary to determine and verify the proposed immune phenotypes.

DHA inhibited tumorigenesis in both the WT and 15-LOX-1 mice groups of the CAC model (**Figure 7**). Tumor numbers per mouse and inflammation scores had similar trends among their groups. Both WT/DHA and 15-LOX-1/DHA mice groups showed similar reductions in inflammation, tumor numbers per mouse, and incidence of larger tumors. The results support our hypothesis and indicate that both 15-LOX-1 expression and dietary DHA inhibited CAC.

We used LC-MS/MS to measure which D-series resolvins play a role in inhibiting tumorigenesis with respect to 15-LOX-1 expression. We found that 17-HDHA and RvD1-5 production are dependent on 15-LOX-1 expression. More specifically, 17-HDHA, RvD1, RvD4, and RvD5 levels further increased with DHA supplementation and 15-LOX-1 expression. On the other hand, RvD2 and RvD3 showed similar increases with 15-LOX-1 expression, regardless of diet type (**Figure 8**). Our study supports a previous study that DSS colitis mouse model treated with 17-HDHA elicit anti-inflammatory and pro-resolution effects (9). As previously reported, RvD1 and RvD2 were involved in preventing colitis (21). In our study, we found significant increase in RvD1, RvD4, and RvD5 production in colitis-associated

tumorigenic model. This study is the first to discover RvD4 as a mediator in CAC. Previous studies have only shown RvD4 in improving thrombosis (80), metastatic prevention (81), and asthma (82). None determined an association with 15-LOX-1. Lastly, RvD5 has only been tested once in a colon model to protect against experimental colitis, and ischemia/reperfusion in a 15-LOX-1 dependent manner (22). However, RvD5 has not been tested in a CAC model. Our results showed the first instance of D-series resolvins (RvD1, RvD4, and RvD5) and their precursor 17-HDHA having an inverse linear regression of correlations with CAC in mice.

As with DHA, supplementation of EPA and/or 15-LOX-1 expression inhibited tumor growth (**Figure 10A-D**). All experimental groups reduced tumor numbers to similar levels and effectively prevented tumors 2 mm or larger from developing. As expected, inflammation scores decreased in all experimental groups at similar levels parallel tumor growth reduction trends. These results are consistent with findings of a previous study investigating EPA in a murine CAC model (83).

Increase in the rate of proliferation and increase in proliferating cells outside the normal zone are predispositions to clinical gastrointestinal cancers (84). Crypts must maintain a balance between proliferation, migration, differentiation, and apoptosis (85). Longer proliferation zones would be conducive of colon cancer. In our study, all experimental groups observed shorter proliferation zones (**Figure 10E**). With 15-LOX-1/EPA establishing the shortest zone, a weak additive effect between 15-LOX-1 and EPA is suggested. The effects of EPA on proliferation has been recently reviewed (86), but we have investigated for the first time colonic cell proliferation in AOM/DSS-induced CAC with dietary EPA.

Lastly, macrophage density was decreased in all experimental groups to similar levels compared to the control group (**Figure 10F**); which supports that EPA is in fact reducing inflammation. Beneficial wound healing characteristics via IL-3 and IL-4 expression and

inhibiting TNF-α and IFN-γ could be modulated by EPA (87). Macrophages could also elicit harmful effects by disrupting the epithelial barrier permeability via IL-6 and nitric oxide, consequently increasing invasion of pathogens (88). However, follow up studies to determine their polarization would give more insight on their function.

Breaking the mechanistic link between inflammation and cancer starts with resolving inflammation (27). Endogenous anti-inflammation and pro-resolution do not elicit the same processes. RvDs are pro-resolving mediators that elicit function with stereochemically selective processes and multitargeted agonist binding (89). This can be observed in their routes of biosynthesis and their ability to interact with receptors. For example, mediators can bind to PMNs and macrophages separately to stimulate resolution (90, 91). More focus is being placed on determining each pro-resolving mediator's stereochemical composition because it will validate their functional interactions with target tissue. In addition, their ability to stimulate inflammatory resolution without host systemic immune suppression supports their capacity as a separate process from endogenous anti-inflammation (92, 93).

Our findings strongly demonstrate the critical role of 15-LOX-1 in resolvin D-series production from DHA. This increase in 17-HDHA and RvD 1-5 by 15-LOX-1 was significantly associated with suppression of chronic colitis. 17-HDHA and RvD 1-5 colonic tissues levels negatively correlated with colonic tumor numbers. Nonetheless, CAC suppression occurred with DHA supplementation with and without 15-LOX-1 transgenic expression and seems to be less dependent on the production of RvDs. Thus, the relationship between the tested resolvins and colonic tumorigenesis seems to be intriguing but complex. RvDs in the context of CAC have not been previously tested. Further in-depth mechanistic studies are therefore needed to be better define the role of resolvins in CAC and colonic tumorigenesis in general.

Bibliography

1. Ferlay, J., I. Soerjomataram, R. Dikshit, S. Eser, C. Mathers, M. Rebelo, D. M. Parkin, D. Forman, and F. Bray. 2015. Cancer incidence and mortality worldwide: sources, methods and major patterns in GLOBOCAN 2012. *Int J Cancer* 136: E359-386.
2. Kim, E. R., and D. K. Chang. 2014. Colorectal cancer in inflammatory bowel disease: the risk, pathogenesis, prevention and diagnosis. *World J Gastroenterol* 20: 9872-9881.
3. Eaden, J. A., K. R. Abrams, and J. F. Mayberry. 2001. The risk of colorectal cancer in ulcerative colitis: a meta-analysis. *Gut* 48: 526-535.
4. Mattar, M. C., D. Lough, M. J. Pishvaian, and A. Charabaty. 2011. Current management of inflammatory bowel disease and colorectal cancer. *Gastrointest Cancer Res* 4: 53-61.
5. Calder, P. C. 2017. Omega-3 fatty acids and inflammatory processes: from molecules to man. *Biochem Soc Trans* 45: 1105-1115.
6. Serini, S., E. Fasano, E. Piccioni, A. R. Cittadini, and G. Calviello. 2011. Dietary n-3 polyunsaturated fatty acids and the paradox of their health benefits and potential harmful effects. *Chem Res Toxicol* 24: 2093-2105.
7. Serini, S., and G. Calviello. 2018. Long-chain omega-3 fatty acids and cancer: any cause for concern? *Curr Opin Clin Nutr Metab Care* 21: 83-89.
8. West, N. J., S. K. Clark, R. K. Phillips, J. M. Hutchinson, R. J. Leicester, A. Belluzzi, and M. A. Hull. 2010. Eicosapentaenoic acid reduces rectal polyp number and size in familial adenomatous polyposis. *Gut* 59: 918-925.
9. Chiu, C. Y., B. Gomolka, C. Dierkes, N. R. Huang, M. Schroeder, M. Purschke, D. Manstein, B. Dangi, and K. H. Weylandt. 2012. Omega-6 docosapentaenoic acid-derived resolvins and 17-hydroxydocosahexaenoic acid modulate macrophage function and alleviate experimental colitis. *Inflamm Res* 61: 967-976.

10. Woodworth, H. L., S. J. McCaskey, D. M. Duriancik, J. F. Clinthorne, I. M. Langohr, E. M. Gardner, and J. I. Fenton. 2010. Dietary fish oil alters T lymphocyte cell populations and exacerbates disease in a mouse model of inflammatory colitis. *Cancer Res* 70: 7960-7969.

11. Terzić, J., S. Grivennikov, E. Karin, and M. Karin. 2010. Inflammation and colon cancer. *Gastroenterology* 138: 2101-2114.e2105.

12. Rogler, G. 2014. Chronic ulcerative colitis and colorectal cancer. *Cancer Lett* 345: 235-241.

13. Bennett, M., and D. W. Gilroy. 2016. Lipid Mediators in Inflammation. *Microbiol Spectr* 4.

14. Serhan, C. N., N. Chiang, and T. E. Van Dyke. 2008. Resolving inflammation: dual anti-inflammatory and pro-resolution lipid mediators. *Nat Rev Immunol* 8: 349-361.

15. Serhan, C. N., and N. Chiang. 2008. Endogenous pro-resolving and anti-inflammatory lipid mediators: a new pharmacologic genus. *Br J Pharmacol* 153 Suppl 1: S200-215.

16. Schwanke, R. C., R. Marcon, A. F. Bento, and J. B. Calixto. 2016. EPA- and DHA-derived resolvins' actions in inflammatory bowel disease. *Eur J Pharmacol* 785: 156-164.

17. Serhan, C. N., N. Chiang, J. Dalli, and B. D. Levy. 2014. Lipid mediators in the resolution of inflammation. *Cold Spring Harb Perspect Biol* 7: a016311.

18. Serhan, C. N., and B. D. Levy. 2018. Resolvins in inflammation: emergence of the pro-resolving superfamily of mediators. *J Clin Invest* 128: 2657-2669.

19. Arita, M., M. Yoshida, S. Hong, E. Tjonahen, J. N. Glickman, N. A. Petasis, R. S. Blumberg, and C. N. Serhan. 2005. Resolvin E1, an endogenous lipid mediator derived

from omega-3 eicosapentaenoic acid, protects against 2,4,6-trinitrobenzene sulfonic acid-induced colitis. *Proc Natl Acad Sci U S A* 102: 7671-7676.

20. Arita, M., F. Bianchini, J. Aliberti, A. Sher, N. Chiang, S. Hong, R. Yang, N. A. Petasis, and C. N. Serhan. 2005. Stereochemical assignment, antiinflammatory properties, and receptor for the omega-3 lipid mediator resolvin E1. *J Exp Med* 201: 713-722.

21. Bento, A. F., R. F. Claudino, R. C. Dutra, R. Marcon, and J. B. Calixto. 2011. Omega-3 fatty acid-derived mediators 17(R)-hydroxy docosahexaenoic acid, aspirin-triggered resolvin D1 and resolvin D2 prevent experimental colitis in mice. *J Immunol* 187: 1957-1969.

22. Gobbetti, T., J. Dalli, R. A. Colas, D. Federici Canova, M. Aursnes, D. Bonnet, L. Alric, N. Vergnolle, C. Deraison, T. V. Hansen, C. N. Serhan, and M. Perretti. 2017. Protectin D1. *Proc Natl Acad Sci U S A* 114: 3963-3968.

23. Il Lee, S., X. Zuo, and I. Shureiqi. 2011. 15-Lipoxygenase-1 as a tumor suppressor gene in colon cancer: is the verdict in? *Cancer Metastasis Rev* 30: 481-491.

24. Serhan, C. N., C. B. Clish, J. Brannon, S. P. Colgan, N. Chiang, and K. Gronert. 2000. Novel functional sets of lipid-derived mediators with antiinflammatory actions generated from omega-3 fatty acids via cyclooxygenase 2-nonsteroidal antiinflammatory drugs and transcellular processing. *J Exp Med* 192: 1197-1204.

25. Hong, S., K. Gronert, P. R. Devchand, R. L. Moussignac, and C. N. Serhan. 2003. Novel docosatrienes and 17S-resolvins generated from docosahexaenoic acid in murine brain, human blood, and glial cells. Autacoids in anti-inflammation. *J Biol Chem* 278: 14677-14687.

26. Gleissman, H., R. Yang, K. Martinod, M. Lindskog, C. N. Serhan, J. I. Johnsen, and P. Kogner. 2010. Docosahexaenoic acid metabolome in neural tumors: identification of cytotoxic intermediates. *FASEB J* 24: 906-915.

27. Tian, R., X. Zuo, J. Jaoude, F. Mao, J. Colby, and I. Shureiqi. 2017. ALOX15 as a suppressor of inflammation and cancer: Lost in the link. *Prostaglandins Other Lipid Mediat* 132: 77-83.

28. Moussalli, M. J., Y. Wu, X. Zuo, X. L. Yang, I. I. Wistuba, M. G. Raso, J. S. Morris, J. L. Bowser, J. D. Minna, R. Lotan, and I. Shureiqi. 2011. Mechanistic contribution of ubiquitous 15-lipoxygenase-1 expression loss in cancer cells to terminal cell differentiation evasion. *Cancer Prev Res (Phila)* 4: 1961-1972.

29. Shureiqi, I., X. Xu, D. Chen, R. Lotan, J. S. Morris, S. M. Fischer, and S. M. Lippman. 2001. Nonsteroidal anti-inflammatory drugs induce apoptosis in esophageal cancer cells by restoring 15-lipoxygenase-1 expression. *Cancer Res* 61: 4879-4884.

30. Jiang, W. G., G. Watkins, A. Douglas-Jones, and R. E. Mansel. 2006. Reduction of isoforms of 15-lipoxygenase (15-LOX)-1 and 15-LOX-2 in human breast cancer. *Prostaglandins Leukot Essent Fatty Acids* 74: 235-245.

31. Sak, M. E., I. Alanbay, A. Rodriguez, T. Gokaslan, M. Borahay, I. Shureiqi, and G. S. Kilic. 2016. The role of 15-lipoxygenase-1 expression and its potential role in the pathogenesis of endometrial hyperplasia and endometrial adenocarcinomas. *Eur J Gynaecol Oncol* 37: 36-40.

32. Philips, B. J., R. Dhir, J. Hutzley, M. Sen, and U. P. Kelavkar. 2008. Polyunsaturated fatty acid metabolizing 15-Lipoxygenase-1 (15-LO-1) expression in normal and tumorigenic human bladder tissues. *Appl Immunohistochem Mol Morphol* 16: 159-164.

33. Hennig, R., T. Kehl, S. Noor, X. Z. Ding, S. M. Rao, F. Bergmann, G. Fürstenberger, M. W. Büchler, H. Friess, P. Krieg, and T. E. Adrian. 2007. 15-lipoxygenase-1 production is lost in pancreatic cancer and overexpression of the gene inhibits tumor cell growth. *Neoplasia* 9: 917-926.

34. Shureiqi, I., K. J. Wojno, J. A. Poore, R. G. Reddy, M. J. Moussalli, S. A. Spindler, J. K. Greenson, D. Normolle, A. A. Hasan, T. S. Lawrence, and D. E. Brenner. 1999. Decreased 13-S-hydroxyoctadecadienoic acid levels and 15-lipoxygenase-1 expression in human colon cancers. *Carcinogenesis* 20: 1985-1995.

35. Nixon, J. B., K. S. Kim, P. W. Lamb, F. G. Bottone, and T. E. Eling. 2004. 15-Lipoxygenase-1 has anti-tumorigenic effects in colorectal cancer. *Prostaglandins Leukot Essent Fatty Acids* 70: 7-15.

36. Heslin, M. J., A. Hawkins, W. Boedefeld, J. P. Arnoletti, A. Frolov, R. Soong, M. M. Urist, and K. I. Bland. 2005. Tumor-associated down-regulation of 15-lipoxygenase-1 is reversed by celecoxib in colorectal cancer. *Ann Surg* 241: 941-946; discussion 946-947.

37. Yuri, M., T. Sasahira, K. Nakai, S. Ishimaru, H. Ohmori, and H. Kuniyasu. 2007. Reversal of expression of 15-lipoxygenase-1 to cyclooxygenase-2 is associated with development of colonic cancer. *Histopathology* 51: 520-527.

38. Zuo, X., J. S. Morris, R. Broaddus, and I. Shureiqi. 2009. 15-LOX-1 transcription suppression through the NuRD complex in colon cancer cells. *Oncogene* 28: 1496-1505.

39. Shureiqi, I., D. Chen, R. S. Day, X. Zuo, F. L. Hochman, W. A. Ross, R. A. Cole, O. Moy, J. S. Morris, L. Xiao, R. A. Newman, P. Yang, and S. M. Lippman. 2010. Profiling lipoxygenase metabolism in specific steps of colorectal tumorigenesis. *Cancer Prev Res (Phila)* 3: 829-838.

40. Zuo, X., and I. Shureiqi. 2013. Eicosanoid profiling in colon cancer: emergence of a pattern. *Prostaglandins Other Lipid Mediat* 104-105: 139-143.

41. Shureiqi, I., W. Jiang, X. Zuo, Y. Wu, J. B. Stimmel, L. M. Leesnitzer, J. S. Morris, H. Z. Fan, S. M. Fischer, and S. M. Lippman. 2003. The 15-lipoxygenase-1 product 13-S-hydroxyoctadecadienoic acid down-regulates PPAR-delta to induce apoptosis in colorectal cancer cells. *Proc Natl Acad Sci U S A* 100: 9968-9973.

42. Shureiqi, I., D. Chen, J. J. Lee, P. Yang, R. A. Newman, D. E. Brenner, R. Lotan, S. M. Fischer, and S. M. Lippman. 2000. 15-LOX-1: a novel molecular target of nonsteroidal anti-inflammatory drug-induced apoptosis in colorectal cancer cells. *J Natl Cancer Inst* 92: 1136-1142.

43. Deguchi, A., S. W. Xing, I. Shureiqi, P. Yang, R. A. Newman, S. M. Lippman, S. J. Feinmark, B. Oehlen, and I. B. Weinstein. 2005. Activation of protein kinase G up-regulates expression of 15-lipoxygenase-1 in human colon cancer cells. *Cancer Res* 65: 8442-8447.

44. Zuo, X., Y. Wu, J. S. Morris, J. B. Stimmel, L. M. Leesnitzer, S. M. Fischer, S. M. Lippman, and I. Shureiqi. 2006. Oxidative metabolism of linoleic acid modulates PPAR-beta/delta suppression of PPAR-gamma activity. *Oncogene* 25: 1225-1241.

45. Shureiqi, I., Y. Wu, D. Chen, X. L. Yang, B. Guan, J. S. Morris, P. Yang, R. A. Newman, R. Broaddus, S. R. Hamilton, P. Lynch, B. Levin, S. M. Fischer, and S. M. Lippman. 2005. The critical role of 15-lipoxygenase-1 in colorectal epithelial cell terminal differentiation and tumorigenesis. *Cancer Res* 65: 11486-11492.

46. Wu, Y., B. Fang, X. Q. Yang, L. Wang, D. Chen, V. Krasnykh, B. Z. Carter, J. S. Morris, and I. Shureiqi. 2008. Therapeutic Molecular Targetingof 15-Lipoxygenase-1 in Colon Cancer. *Mol Ther* 16: 886-892.

47. Zuo, X., Z. Peng, Y. Wu, M. J. Moussalli, X. L. Yang, Y. Wang, J. Parker-Thornburg, J. S. Morris, R. R. Broaddus, S. M. Fischer, and I. Shureiqi. 2012. Effects of gut-targeted 15-LOX-1 transgene expression on colonic tumorigenesis in mice. *J Natl Cancer Inst* 104: 709-716.

48. Mao, F., M. Xu, X. Zuo, J. Yu, W. Xu, M. J. Moussalli, E. Elias, H. S. Li, S. S. Watowich, and I. Shureiqi. 2015. 15-Lipoxygenase-1 suppression of colitis-associated colon cancer through inhibition of the IL-6/STAT3 signaling pathway. *FASEB J* 29: 2359-2370.

49. Fletcher, R., Y. J. Wang, R. E. Schoen, O. J. Finn, J. Yu, and L. Zhang. 2018. Colorectal cancer prevention: Immune modulation taking the stage. *Biochim Biophys Acta Rev Cancer* 1869: 138-148.

50. Eltweri, A. M., A. L. Thomas, M. Metcalfe, P. C. Calder, A. R. Dennison, and D. J. Bowrey. 2017. Potential applications of fish oils rich in omega-3 polyunsaturated fatty acids in the management of gastrointestinal cancer. *Clin Nutr* 36: 65-78.

51. Paixão, E. M. D. S., A. C. M. Oliveira, N. Pizato, M. I. Muniz-Junqueira, K. G. Magalhães, E. Y. Nakano, and M. K. Ito. 2017. The effects of EPA and DHA enriched fish oil on nutritional and immunological markers of treatment naïve breast cancer patients: a randomized double-blind controlled trial. *Nutr J* 16: 71.

52. Wang, C. C., C. J. Yang, L. H. Wu, H. C. Lin, Z. H. Wen, and C. H. Lee. 2018. Eicosapentaenoic acid reduces indoleamine 2,3-dioxygenase 1 expression in tumor cells. *Int J Med Sci* 15: 1296-1303.

53. Kim, M., C. Galan, A. A. Hill, W. J. Wu, H. Fehlner-Peach, H. W. Song, D. Schady, M. L. Bettini, K. W. Simpson, R. S. Longman, D. R. Littman, and G. E. Diehl. 2018. Critical Role for the Microbiota in CX. *Immunity* 49: 151-163.e155.

54. Hamamoto, N., K. Maemura, I. Hirata, M. Murano, S. Sasaki, and K. Katsu. 1999. Inhibition of dextran sulphate sodium (DSS)-induced colitis in mice by intracolonically administered antibodies against adhesion molecules (endothelial leucocyte adhesion molecule-1 (ELAM-1) or intercellular adhesion molecule-1 (ICAM-1)). *Clin Exp Immunol* 117: 462-468.

55. Zuo, X., Y. Deguchi, W. Xu, Y. Liu, H. S. Li, D. Wei, R. Tian, W. Chen, M. Xu, Y. Yang, S. Gao, J. C. Jaoude, F. Liu, S. P. Chrieki, M. J. Moussalli, M. Gagea, M. M. Sebastian, X. Zheng, D. Tan, R. Broaddus, J. Wang, N. J. Ajami, A. G. Swennes, S. S. Watowich, and I. Shureiqi. 2019. PPARD and Interferon Gamma Promote Transformation of Gastric Progenitor Cells and Tumorigenesis in Mice. *Gastroenterology* 157: 163-178.

56. Liu, Y., Y. Deguchi, R. Tian, D. Wei, L. Wu, W. Chen, W. Xu, M. Xu, F. Liu, S. Gao, J. C. Jaoude, S. P. Chrieki, M. J. Moussalli, M. Gagea, J. Morris, R. R. Broaddus, X. Zuo, and I. Shureiqi. 2019. Pleiotropic Effects of PPARD Accelerate Colorectal Tumorigenesis, Progression, and Invasion. *Cancer Res* 79: 954-969.

57. Yang, P., D. Chan, E. Felix, T. Madden, R. D. Klein, I. Shureiqi, X. Chen, A. J. Dannenberg, and R. A. Newman. 2006. Determination of endogenous tissue inflammation profiles by LC/MS/MS: COX- and LOX-derived bioactive lipids. *Prostaglandins Leukot Essent Fatty Acids* 75: 385-395.

58. Kutzner, L., K. M. Rund, A. I. Ostermann, N. M. Hartung, J. M. Galano, L. Balas, T. Durand, M. S. Balzer, S. David, and N. H. Schebb. 2019. Development of an Optimized LC-MS Method for the Detection of Specialized Pro-Resolving Mediators in Biological Samples. *Front Pharmacol* 10: 169.

59. Colas, R. A., M. Shinohara, J. Dalli, N. Chiang, and C. N. Serhan. 2014. Identification and signature profiles for pro-resolving and inflammatory lipid mediators in human tissue. *Am J Physiol Cell Physiol* 307: C39-54.

60. Liu, B., W. A. Khan, Y. A. Hannun, J. Timar, J. D. Taylor, S. Lundy, I. Butovich, and K. V. Honn. 1995. 12(S)-hydroxyeicosatetraenoic acid and 13(S)-hydroxyoctadecadienoic acid regulation of protein kinase C-alpha in melanoma cells: role of receptor-mediated hydrolysis of inositol phospholipids. *Proc Natl Acad Sci U S A* 92: 9323-9327.

61. Müller, K., M. Siebert, M. Heidt, F. Marks, P. Krieg, and G. Fürstenberger. 2002. Modulation of epidermal tumor development caused by targeted overexpression of epidermis-type 12S-lipoxygenase. *Cancer Res* 62: 4610-4616.

62. Paintlia, A. S., M. K. Paintlia, I. Singh, and A. K. Singh. 2006. IL-4-induced peroxisome proliferator-activated receptor gamma activation inhibits NF-kappaB trans activation in central nervous system (CNS) glial cells and protects oligodendrocyte progenitors under neuroinflammatory disease conditions: implication for CNS-demyelinating diseases. *J Immunol* 176: 4385-4398.

63. Wen, Y., J. Gu, S. K. Chakrabarti, K. Aylor, J. Marshall, Y. Takahashi, T. Yoshimoto, and J. L. Nadler. 2007. The role of 12/15-lipoxygenase in the expression of interleukin-6 and tumor necrosis factor-alpha in macrophages. *Endocrinology* 148: 1313-1322.

64. Ricote, M., J. S. Welch, and C. K. Glass. 2000. Regulation of macrophage gene expression by the peroxisome proliferator-activated receptor-gamma. *Horm Res* 54: 275-280.

65. Okamoto, R., and M. Watanabe. 2016. Role of epithelial cells in the pathogenesis and treatment of inflammatory bowel disease. *J Gastroenterol* 51: 11-21.

66. Collin, M., and V. Bigley. 2018. Human dendritic cell subsets: an update. *Immunology* 154: 3-20.

67. Colby, J. K., J. Jaoude, F. Liu, and I. Shureiqi. 2018. Oxygenated lipid signaling in tumor-associated macrophages-focus on colon cancer. *Cancer Metastasis Rev* 37: 289-315.

68. Stables, M. J., S. Shah, E. B. Camon, R. C. Lovering, J. Newson, J. Bystrom, S. Farrow, and D. W. Gilroy. 2011. Transcriptomic analyses of murine resolution-phase macrophages. *Blood* 118: e192-208.

69. Jones, H. R., C. T. Robb, M. Perretti, and A. G. Rossi. 2016. The role of neutrophils in inflammation resolution. *Semin Immunol* 28: 137-145.

70. Schuster, S., D. Cabrera, M. Arrese, and A. E. Feldstein. 2018. Triggering and resolution of inflammation in NASH. *Nat Rev Gastroenterol Hepatol* 15: 349-364.

71. Miles, K., D. J. Clarke, W. Lu, Z. Sibinska, P. E. Beaumont, D. J. Davidson, T. A. Barr, D. J. Campopiano, and M. Gray. 2009. Dying and necrotic neutrophils are anti-inflammatory secondary to the release of alpha-defensins. *J Immunol* 183: 2122-2132.

72. Lu, J., Q. Cao, D. Zheng, Y. Sun, C. Wang, X. Yu, Y. Wang, V. W. Lee, G. Zheng, T. K. Tan, X. Wang, S. I. Alexander, and D. C. Harris. 2013. Discrete functions of M2a and M2c macrophage subsets determine their relative efficacy in treating chronic kidney disease. *Kidney Int* 84: 745-755.

73. McArthur, S., T. Gobbetti, D. H. Kusters, C. P. Reutelingsperger, R. J. Flower, and M. Perretti. 2015. Definition of a Novel Pathway Centered on Lysophosphatidic Acid To Recruit Monocytes during the Resolution Phase of Tissue Inflammation. *J Immunol* 195: 1139-1151.

74. Gobbetti, T., S. M. Coldewey, J. Chen, S. McArthur, P. le Faouder, N. Cenac, R. J. Flower, C. Thiemermann, and M. Perretti. 2014. Nonredundant protective properties of FPR2/ALX in polymicrobial murine sepsis. *Proc Natl Acad Sci U S A* 111: 18685-18690.

75. Harrison, O. J., N. Srinivasan, J. Pott, C. Schiering, T. Krausgruber, N. E. Ilott, and K. J. Maloy. 2015. Epithelial-derived IL-18 regulates Th17 cell differentiation and Foxp3^{+} Treg cell function in the intestine. *Mucosal Immunol* 8: 1226-1236.

76. Mottet, C., H. H. Uhlig, and F. Powrie. 2003. Cutting edge: cure of colitis by CD4+CD25+ regulatory T cells. *J Immunol* 170: 3939-3943.

77. Smillie, C. S., M. Biton, J. Ordovas-Montanes, K. M. Sullivan, G. Burgin, D. B. Graham, R. H. Herbst, N. Rogel, M. Slyper, J. Waldman, M. Sud, E. Andrews, G. Velonias, A. L. Haber, K. Jagadeesh, S. Vickovic, J. Yao, C. Stevens, D. Dionne, L. T. Nguyen, A. C. Villani, M. Hofree, E. A. Creasey, H. Huang, O. Rozenblatt-Rosen, J. J. Garber, H. Khalili, A. N. Desch, M. J. Daly, A. N. Ananthakrishnan, A. K. Shalek, R. J. Xavier, and A. Regev. 2019. Intra- and Inter-cellular Rewiring of the Human Colon during Ulcerative Colitis. *Cell* 178: 714-730.e722.

78. Reynoso, E. D., K. G. Elpek, L. Francisco, R. Bronson, A. Bellemare-Pelletier, A. H. Sharpe, G. J. Freeman, and S. J. Turley. 2009. Intestinal tolerance is converted to autoimmune enteritis upon PD-1 ligand blockade. *J Immunol* 182: 2102-2112.

79. Pauken, K. E., C. E. Nelson, T. Martinov, J. A. Spanier, J. R. Heffernan, N. L. Sahli, C. F. Quarnstrom, K. C. Osum, J. M. Schenkel, M. K. Jenkins, B. R. Blazar, V. Vezys, and B. T. Fife. 2015. Cutting edge: identification of autoreactive CD4+ and CD8+ T cell subsets resistant to PD-1 pathway blockade. *J Immunol* 194: 3551-3555.

80. Cherpokova, D., C. C. Jouvene, S. Libreros, E. P. DeRoo, L. Chu, X. de la Rosa, P. C. Norris, D. D. Wagner, and C. N. Serhan. 2019. Resolvin D4 attenuates the severity of pathological thrombosis in mice. *Blood* 134: 1458-1468.

81. Panigrahy, D., A. Gartung, J. Yang, H. Yang, M. M. Gilligan, M. L. Sulciner, S. S. Bhasin, D. R. Bielenberg, J. Chang, B. A. Schmidt, J. Piwowarski, A. Fishbein, D. Soler-Ferran, M. A. Sparks, S. J. Staffa, V. Sukhatme, B. D. Hammock, M. W. Kieran, S. Huang, M. Bhasin, C. N. Serhan, and V. P. Sukhatme. 2019. Preoperative stimulation of resolution and inflammation blockade eradicates micrometastases. *J Clin Invest* 129: 2964-2979.

82. Fussbroich, D., R. A. Colas, O. Eickmeier, J. Trischler, S. P. Jerkic, K. Zimmermann, A. Göpel, T. Schwenger, A. Schaible, D. Henrich, P. Baer, S. Zielen, J. Dalli, C. Beermann, and R. Schubert. 2020. A combination of LCPUFA ameliorates airway inflammation in asthmatic mice by promoting pro-resolving effects and reducing adverse effects of EPA. *Mucosal Immunol*.

83. Piazzi, G., G. D'Argenio, A. Prossomariti, V. Lembo, G. Mazzone, M. Candela, E. Biagi, P. Brigidi, P. Vitaglione, V. Fogliano, L. D'Angelo, C. Fazio, A. Munarini, A. Belluzzi, C. Ceccarelli, P. Chieco, T. Balbi, P. M. Loadman, M. A. Hull, M. Romano, F. Bazzoli, and L. Ricciardiello. 2014. Eicosapentaenoic acid free fatty acid prevents and suppresses colonic neoplasia in colitis-associated colorectal cancer acting on Notch signaling and gut microbiota. *Int J Cancer* 135: 2004-2013.

84. Eastwood, G. L. 1995. A review of gastrointestinal epithelial renewal and its relevance to the development of adenocarcinomas of the gastrointestinal tract. *J Clin Gastroenterol* 21 Suppl 1: S1-11.

85. Shanmugathasan, M., and S. Jothy. 2000. Apoptosis, anoikis and their relevance to the pathobiology of colon cancer. *Pathol Int* 50: 273-279.

86. Senatorov, I. S., and N. H. Moniri. 2018. The role of free-fatty acid receptor-4 (FFA4) in human cancers and cancer cell lines. *Biochem Pharmacol* 150: 170-180.

87. Seno, H., H. Miyoshi, S. L. Brown, M. J. Geske, M. Colonna, and T. S. Stappenbeck. 2009. Efficient colonic mucosal wound repair requires Trem2 signaling. *Proc Natl Acad Sci U S A* 106: 256-261.

88. Du Plessis, J., H. Vanheel, C. E. Janssen, L. Roos, T. Slavik, P. I. Stivaktas, M. Nieuwoudt, S. G. van Wyk, W. Vieira, E. Pretorius, M. Beukes, R. Farré, J. Tack, W. Laleman, J. Fevery, F. Nevens, T. Roskams, and S. W. Van der Merwe. 2013. Activated intestinal macrophages in patients with cirrhosis release NO and IL-6 that may disrupt intestinal barrier function. *J Hepatol* 58: 1125-1132.

89. Serhan, C. N. 2014. Pro-resolving lipid mediators are leads for resolution physiology. *Nature* 510: 92-101.

90. Schwab, J. M., N. Chiang, M. Arita, and C. N. Serhan. 2007. Resolvin E1 and protectin D1 activate inflammation-resolution programmes. *Nature* 447: 869-874.

91. Chiang, N., G. Fredman, F. Bäckhed, S. F. Oh, T. Vickery, B. A. Schmidt, and C. N. Serhan. 2012. Infection regulates pro-resolving mediators that lower antibiotic requirements. *Nature* 484: 524-528.

92. Spite, M., L. V. Norling, L. Summers, R. Yang, D. Cooper, N. A. Petasis, R. J. Flower, M. Perretti, and C. N. Serhan. 2009. Resolvin D2 is a potent regulator of leukocytes and controls microbial sepsis. *Nature* 461: 1287-1291.

93. Oh, S. F., P. S. Pillai, A. Recchiuti, R. Yang, and C. N. Serhan. 2011. Pro-resolving actions and stereoselective biosynthesis of 18S E-series resolvins in human leukocytes and murine inflammation. *J Clin Invest* 121: 569-581.

Vita

Jonathan Chuck Jaoude was born in Houston, Texas, the son of Chuck and Eliana Jaoude. After completing his work at Memorial High School, Houston, Texas in 2011, he entered Baylor University in Waco, Texas. He received the degree of Bachelor of Science with a major in biology and French from Baylor in May 2015. In June of 2015, he entered Baylor University Graduate School in Waco, Texas. He received the degree of Master of Arts with a major in biology in May 2016. For the next year, he worked as a research assistant in the Department of GI Medical Oncology at The University of Texas MD Anderson Cancer. In August of 2017, he entered The University of Texas MD Anderson Cancer Center UTHealth Graduate School of Biomedical Sciences.

Permanent address:

9230 Larston Street

Houston, Texas 77055